Evolutionary Conservation of a GPCR-Independent Mechanism of Trimeric G Protein Activation

Brantley D. Coleman,[1,†] Arthur Marivin,[1,†] Kshitij Parag-Sharma,[1] Vincent DiGiacomo,[1] Seongseop Kim,[2] Judy S. Pepper,[2] Jason Casler,[1] Lien T. Nguyen,[1] Michael R. Koelle,[2] Mikel Garcia-Marcos[*,1]

[1]Department of Biochemistry, Boston University School of Medicine

[2]Department of Molecular Biophysics and Biochemistry, Yale University School of Medicine

[†]These authors contributed equally to this work.

***Corresponding author:** E-mail: mgm1@bu.edu.

Associate editor: Joel Dudley

Abstract

Trimeric G protein signaling is a fundamental mechanism of cellular communication in eukaryotes. The core of this mechanism consists of activation of G proteins by the guanine-nucleotide exchange factor (GEF) activity of G protein coupled receptors. However, the duration and amplitude of G protein-mediated signaling are controlled by a complex network of accessory proteins that appeared and diversified during evolution. Among them, nonreceptor proteins with GEF activity are the least characterized. We recently found that proteins of the ccdc88 family possess a Gα-binding and activating (GBA) motif that confers GEF activity and regulates mammalian cell behavior. A sequence similarity-based search revealed that ccdc88 genes are highly conserved across metazoa but the GBA motif is absent in most invertebrates. This prompted us to investigate whether the GBA motif is present in other nonreceptor proteins in invertebrates. An unbiased bioinformatics search in *Caenorhabditis elegans* identified GBAS-1 (GBA and SPK domain containing-1) as a GBA motif-containing protein with homologs only in closely related worm species. We demonstrate that GBAS-1 has GEF activity for the nematode G protein GOA-1 and that the two proteins are coexpressed in many cells of living worms. Furthermore, we show that GBAS-1 can activate mammalian Gα-subunits and provide structural insights into the evolutionarily conserved determinants of the GBA–G protein interface. These results demonstrate that the GBA motif is a functional GEF module conserved among highly divergent proteins across evolution, indicating that the GBA-Gα binding mode is strongly constrained under selective pressure to mediate receptor-independent G protein activation in metazoans.

***Key words:* C. elegans, GOA-1, DAPLE, Girdin, Ric-8.**

Article

Introduction

Both unicellular and multicellular organisms require a molecular system to perceive stimuli from the environment and transduce them inside the cell to elicit an adequate adaptive response. In multicellular organisms, these systems have evolved into complex networks of signaling pathways. One of the main signaling mechanisms in eukaryotes is that mediated by trimeric G proteins. Trimeric G proteins are composed of an α subunit (Gα) with GTPase activity and an obligatory heterodimer of β and γ subunits (Gβγ) (Gilman 1987; Morris and Malbon 1999). In the classical view of this signal transduction mechanism, the first step consists of an extracellular signal acting on G protein-coupled receptors (GPCRs) at the plasma membrane. GPCRs have seven-transmembrane domains (7-TM) and undergo a conformational change upon activation that is transmitted to the inner side of the plasma membrane, where they couple to trimeric G proteins (Rosenbaum et al. 2009). Ligand-bound GPCRs act as guanine-nucleotide exchange factors (GEFs) that activate trimeric G proteins by promoting the exchange of guanosine diphosphate (GDP) for guanosine-5′-triphosphate (GTP) on Gα. Upon GTP binding, Gα changes conformation and dissociates from Gβγ. Both Gα-GTP and free Gβγ activate a wide range of downstream effectors to elicit cellular responses. Signaling is terminated when Gα hydrolyzes GTP to GDP and the cycle is completed by reassociation of inactive Gα-GDP with Gβγ.

This cycle of reactions, commonly referred to as the "G protein cycle," is conserved essentially through all eukaryotic taxa and is believed to be present in the last eukaryotic common ancestor (de Mendoza et al. 2014). However, there is a marked lineage-specific diversification of this system. For example, the number of GPCRs expanded dramatically in metazoans and the number of different Gα, Gβ, and Gγ subunits are also increased in amorpheans and plants compared with other evolutionary clades (Anantharaman et al. 2010; de Mendoza et al. 2014).

The complexity of the trimeric G protein signaling network is further increased by the existence of accessory proteins that regulate either GPCRs or G proteins (Sato et al. 2006). Among these accessory proteins, regulators of the activity of Gα subunits play a critical role because they control the lifetime of GTP-bound Gα, which determines the duration and intensity of signaling. The best characterized of these accessory proteins are GTPase activating proteins (GAPs) (Dohlman and Thorner 1997; De Vries et al. 2000; Ross and Wilkie 2000)

and guanine-nucleotide dissociation inhibitors (GDIs) (Willard et al. 2004; Blumer et al. 2012). Although both GAPs and GDIs work as inhibitors of Gα subunits, the molecular mechanisms that they use are different: GAPs accelerate the intrinsic GTPase activity of Gα whereas GDIs block nucleotide exchange. These G protein regulators are modular, that is, signature motifs or domains are sufficient for their G protein regulatory function. GAPs contain a regulator of G protein signaling (RGS) domain of approximately 120 aa (Ross and Wilkie 2000) and GDIs a GoLoco/GPR motif of 20–30 aa (Willard et al. 2004; Blumer et al. 2012).

The appearance and diversification of these accessory proteins during evolution are also lineage-specific. For example, GoLoco/GPR proteins are primarily found in metazoans (de Mendoza et al. 2014). On the other hand, GAPs of the RGS family are present in all eukaryotes but their number is increased in amorpheans and plants, which correlates with the increased diversification of trimeric G protein subunits in these taxa (Anantharaman et al. 2010; de Mendoza et al. 2014). A different mode of RGS diversification is the appearance of RGS-like proteins in metazoans (de Mendoza et al. 2014). RGS-like domains conserve the architecture of RGS domains and the ability to bind G proteins while lacking GAP activity (Ross and Wilkie 2000). Yet another example of RGS diversification is related to their modular composition: RGS domains are frequently embedded in proteins with additional functional domains and some domain architectures are present only in certain taxa (Anantharaman et al. 2010; de Mendoza et al. 2014). The R7 family of RGS proteins, for example, contains DEP and GGL domains (Drenan et al. 2005; Cheever et al. 2008) and is only present in amorphea (de Mendoza et al. 2014).

A third group of accessory proteins that regulate the activity of Gα proteins are nonreceptor GEFs. Nonreceptor GEFs mimic the action of GPCRs but they are cytoplasmic factors instead on membrane receptors (Siderovski and Willard 2005; Sato et al. 2006; Garcia-Marcos et al. 2015; Papasergi et al. 2015). They are the least characterized G protein regulators, in part because of the lack of a signature domain or motif that defines them. This has hampered both the development of tools to characterize their biological functions and the systematic characterization of their evolution as a group. For example, Ric8, one of the best characterized nonreceptor GEFs, is present across amorpheans and in some heterokonts (de Mendoza et al. 2014). However, the lack of sequence similarity with other nonreceptors GEFs makes it difficult to assess whether this pattern of distribution across evolutionary clades is common to all nonreceptors GEFs or unique to this particular protein and close homologs. In addition, the lack of a defined functional domain and knowledge of the structural determinants required for the GEF activity of Ric8 casts doubt over inferences of G protein regulatory activity based solely on the sequence similarity of distant orthologs. Therefore, it would be important to identify signature domains or motifs of other nonreceptor GEFs and characterize their conservation in different evolutionary clades to improve our understanding of the evolutionary history of this class of G protein regulators as a whole.

It has been recently reported that a signature Gα binding and activating (GBA) motif identified in some mammalian proteins and synthetic peptides possesses GEF activity toward Gαi proteins (Gαi1, Gαi2, and Gαi3) (Johnston et al. 2005; Austin et al. 2008; Garcia-Marcos et al. 2009, 2015; Garcia-Marcos, Kietrsunthorn, et al. 2011; Aznar et al. 2015). This is the first instance in which the GEF activity of nonreceptor proteins has been directly linked to a defined sequence. The GBA motif is 15–25 aa long and the crystallization of a synthetic GBA-like peptide has provided insights into the structural basis of its binding to Gα (Johnston et al. 2005). GIV and DAPLE are the best characterized nonreceptor GEFs with a GBA motif and the only ones for which the biological function of the GBA motif in cell signaling has been established (Ghosh et al. 2008, 2010; Garcia-Marcos et al. 2009, 2012; Aznar et al. 2015). GPCR-independent G protein activation by GIV and DAPLE is physiologically important because its dysregulation is associated with diseases such as cancer, fibrosis or nephropathy (Ghosh et al. 2010; Garcia-Marcos, Jung, et al. 2011; Lopez-Sanchez et al. 2014; Wang et al. 2014; Aznar et al. 2015).

GIV and DAPLE belong to the same family of proteins, ccdc88. To gain insights into the evolutionary conservation of the GPCR-independent mechanism of G protein activation mediated by GBA proteins, we systematically analyzed ccdc88 orthologs for the presence of a GBA motif. Our analyses (see below) revealed that ccdc88 proteins are widely present across metazoans but that the GBA motif is absent in most invertebrates whereas present in almost all the vertebrate orthologs analyzed. This prompted us to search for other proteins with a GBA motif in invertebrates and test their ability to functionally couple to G proteins. Here, we report the identification of a GBA motif in a *Caenorhabditis elegans* protein completely unrelated to the ccdc88 family and with orthologs only in some other nematode species. This protein acts as a GEF not only for the cognate Gα in *C. elegans* (i.e., GOA-1) but also for mammalian Gα proteins. This is the first validation of a nonreceptor GEF of the GBA family in invertebrates, which demonstrates that the GBA motif is a functional GEF module conserved in evolutionarily divergent proteins and that this mechanism of receptor-independent G protein activation appeared at least 300 Ma. This work also sets the basis for the identification and subclassification of novel nonreceptor GEFs in different species across evolution.

Results and Discussion

Evolutionary Conservation of the GBA Motif in the ccdc88 Family

GIV and DAPLE belong to the ccdc88 family, which is composed of three members in humans: ccdc88a (GIV), ccdc88b (GIPIE), and ccdc88c (DAPLE) (Enomoto et al. 2006; Matsushita et al. 2011; Aznar et al. 2015). These proteins are classified into the same family because the N-terminal region (~1,400 aa) is highly conserved among them. On the other hand, the C-terminal region of the three proteins is highly divergent: ccdc88b (GIPIE) has a very short C-terminal region and the longer C-terminal regions (~400–600 aa) of

GIV and DAPLE are very different to each other (only ~15% identity). Interestingly, the conserved GBA motifs of GIV and DAPLE are located within their divergent C-terminal regions (Aznar et al. 2015), suggesting functional conservation due to selective pressure. To further investigate the evolutionary history of the GBA motif in the ccdc88 family, we carried out a systematic phylogenetic analysis of the ccdc88 family (fig. 1). We found ccdc88 orthologs in 82 of 85 metazoan species and three of five holozoans (fig. 1 and supplementary table S1, Supplementary Material online). Among the rest of the amorpheans investigated, only one species (*Spizellomyces punctatus*) of 11 had a ccdc88 protein (fig. 1 and supplementary table S1, Supplementary Material online), although it should be noted that the statistical parameters of the query results were of much lower confidence than for the metazoan counterparts (e.g., BLASTp *E* values of 10^{-6} for *S. punctatus* vs. 10^{-179} for *Danio rerio*). Similarly, three of the seven bikonts investigated displayed ccdc88 orthologs with low statistical confidence. Analysis of the 87 metazoan species revealed that the number of orthologs per species increased from a median of one (range 0–1) in invertebrates to a median of 3 (range 2–9) in vertebrates (fig. 1). Importantly, the GBA motif was absent from the majority of invertebrate orthologs (present only in 5 of 43 or 11.6% of the species) whereas it was present in at least one ortholog of almost all the vertebrate species (37 of 38 or 97.3% of the species) (fig. 1). A median of two ccdc88 orthologs per species contained a GBA motif (fig. 1).

Taken together, these observations indicate that the ccdc88 family appeared in evolution at least at the level of unicellular holozoans. In metazoans, the ccdc88 family diversified by gene duplication in the transition from invertebrates to vertebrates. This transition also marked an inflexion point for the conservation of the GBA motif. Although the GBA motif was present in early branching metazoans like sponges, it was lost in the majority of invertebrates and preserved in almost all vertebrates.

Identification of GBAS-1, a Unique GBA Motif-Containing Protein in *C. elegans*

One possible explanation for the absence of the GBA motif in many ccdc88 proteins of invertebrates is that the motif is not functional (i.e., does not bind/regulate G proteins) in invertebrates and easily lost under selective pressure. This prompted us to investigate whether other proteins in invertebrates contain a functional GBA motif and thereby test whether this sequence motif works as an independent G protein regulatory module across metazoans. For this, we used all GBA sequences that have been experimentally validated to bind and activate G proteins to create and implement a position-specific scoring matrix (PSSM) in ScanSite3. This PSSM was used to search the proteome of the nematode *C. elegans*, an extensively characterized invertebrate model organism with a well-annotated proteome. *Caenorhabditis elegans* is also one of the invertebrate species with a ccdc88 ortholog lacking the GBA motif, therefore representing a good system to test whether a non-ccdc88 protein with a GBA motif can modulate one of its cognate G proteins. The best fit (top scoring) motif of this search was found in the uncharacterized protein F59H5.1 (fig. 2A). The 0.056 score for the putative GBA motif in F59H5.1 corresponds to a 0.055 percentile of all ranked scores in the search (supplementary fig. S1, Supplementary Material online), which is statistically significant based on the high stringency cutoff (0.2 percentile) of ScanSite3. Moreover, the overall distribution of scores for motifs identified in the search is dramatically shifted toward high values (supplementary fig. S1, Supplementary Material online), which indicates that sequences similar to the GBA motif are very infrequent in this data set. Taken together, these results indicate that F59H5.1 is a high probability candidate for the presence of a bona fide GBA motif. Interestingly, this protein has been previously reported as a hit in a yeast two-hybrid screen for binding proteins of the *C. elegans* Gα protein GOA-1 (Cuppen et al. 2003). For these reasons, we focused our efforts on characterizing F59H5.1, although it is possible that other high scoring candidates from our search are also nonreceptor GEFs of the same class.

The F59H5.1 protein features two domains of unknown function (DUFs). One is an SPK domain (domain in SET and PHD-containing proteins and protein Kinases a.k.a. DUF545), which is found only in nematodes, and the other one is a DUF2890 domain, which is characteristic of adenoviruses of vertebrates. The putative GBA motif sequence is embedded within the DUF2890 domain and conforms with the core 7 aa consensus [ψ]-[T]-[ψ]-[x]-[D/E]-[F]-[ψ] (where "x" is any residue and ψ is a hydrophobic residue) found in all previously reported GBA proteins (fig. 2A). Based on the presence of these features we named this protein GBAS-1 for "GBA and SPK containing-1." We did not find a GBA motif in any of the 280 DUF2890 sequences listed in the Pfam database and none of the known GEFs with a GBA motif in vertebrates contained a DUF2890 domain (not shown). Moreover, a phylogenetic analysis revealed that GBAS-1 has homologs only in two nematode species closely related to *C. elegans* but not in other metazoans (fig. 2B). We found that one of the GBAS-1 homologs contained a GBA motif (^{1100}VTVKEFL^{1106} in CRE20827 of *Caenorhabditis remanei*) and a similar domain architecture, with three SPK domains in the N-terminal region and the GBA motif close to the C-terminus (fig. 2B). Although this suggests that the GBA motif could have appeared in a common ancestor of nematodes and conserved in some nematode species whereas lost in others, the current set of sequenced nematode genomes does not provide the power to assess this. Regardless of this, the most likely explanation for the appearance of a GBA motif in GBAS-1-related proteins and ccdc88 proteins is convergent evolution because these are completely unrelated proteins and the GBA motif is a short. A more intricate but still possible scenario is that GBAS-1 acquired the GBA motif by domain-shuffling from an ancestral ccdc88 protein (i.e., the GBA motif was lost in ccdc88 in *C. elegans* whereas it emerged in GBAS-1). The restricted presence of GBAS-1 in *Caenorhabditis* but not other species could be related to an adaptation to the increased complexity of the G protein signaling network. For example, *C. elegans* contains almost double the number of GPCRs (~1,400) and Gα subunits (24) than *Homo sapiens*.

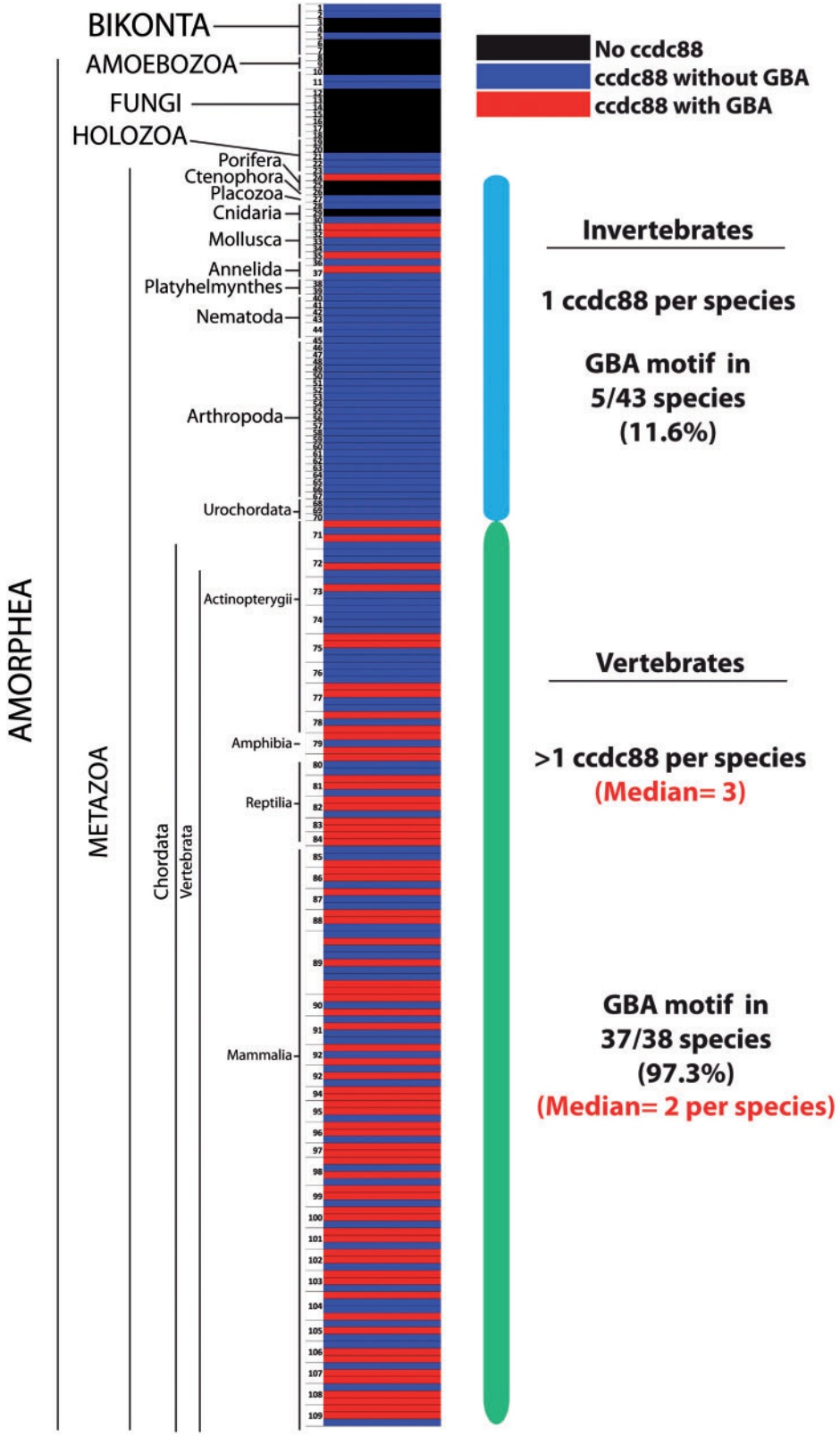

Fig. 1. ccdc88 proteins are present across metazoans but the GBA motif is absent in the majority of invertebrates. Sequences of 201 ccdc88 orthologs in 109 species were analyzed for the presence of a GBA motif as described in Materials and Methods. Each species is indicated by a number on the left of the colored column (a full list of the species names corresponding to each number is provided in supplementary table S1, Supplementary Material online). Each colored row in the central column represents one protein (a full list of the corresponding database accession numbers is provided in supplementary table S1, Supplementary Material online). Blue and red indicate absence or presence, respectively, of a GBA motif. Those species in which no ccdc88 protein was found are indicated in black.

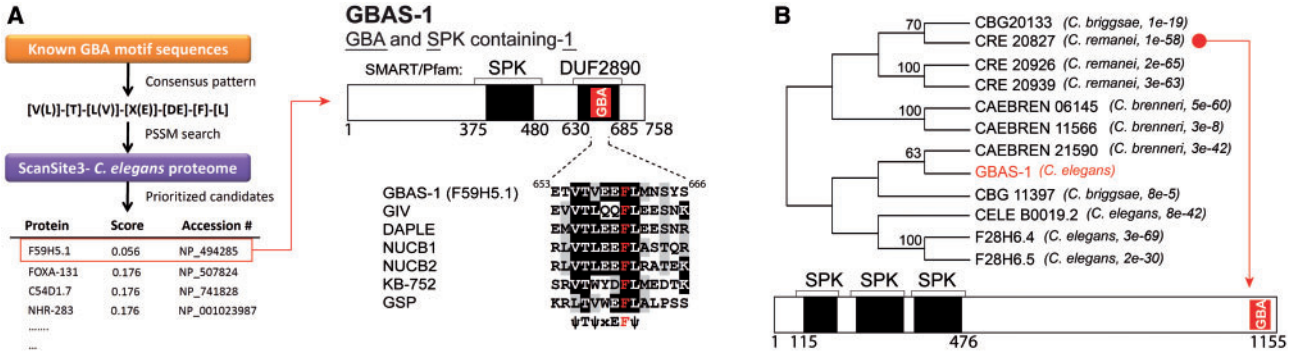

Fig. 2. Identification of GBAS-1 as a unique GBA motif-containing protein in *Caenorhabditis elegans*. (*A*) Bionformatics search for GBA motif-containing proteins in *C. elegans* identifies GBAS-1. Left: Sequences of known GBA motifs were used to search the *C. elegans* proteome as described in Materials and Methods. The uncharacterized protein F59H5.1 was the top scoring candidate. We named the top candidate (F59H5.1) GBAS-1 for GBA and SPK containing-1. Right: Bar diagram of GBAS-1 domains with the predicted GBA motif in red. The alignment of the putative GBA motif of GBAS-1 with the known GBA sequences of GIV, DAPLE, NUCB1, and NUCB2 proteins and the synthetic KB-752 and GSP peptides is shown below along with a consensus sequence (ψ, hydrophobic; x, any). The invariable phenylalanine (F) is in red. (*B*) GBAS-1-related proteins are restricted to nematode species. A cladogram of GBAS-1-related sequences was generated as described in Materials and Methods. Consensus tree inferred from 500 replicates with bootstrap values shown for branching reproduced in > 60% of replicates. Species and BLAST *E* value are indicated beside protein name. Bottom: Bar diagram of CRE20827 domains, which include three SPK domains and a GBA motif.

Taken together, these results indicate that GBAS-1 is a putative nonreceptor GEF of the GBA class but evolutionarily unrelated to previously described GEFs in vertebrates.

GBAS-1 Is Coexpressed with GOA-1 in *C. elegans* Cells and Binds Directly to GOA-1 *In Vitro*

As mentioned above, GBAS-1 was previously found as a hit in a yeast two-hybrid screen for GOA-1 binding proteins (Cuppen et al. 2003). However, yeast two-hybrid assays are prone to yield false positive hits and the GBAS-1/GOA-1 interaction was not confirmed by alternative and more direct methods. Nevertheless, the same study (Cuppen et al. 2003) reported that GBAS-1 does not interact with any other Gα subunit of *C. elegans* in yeast two-hybrid assays, suggesting that, if the identified interaction is a true positive, it is likely be specific for GOA-1. We set out to validate whether GBAS-1 interacts with GOA-1 and if so, whether the interaction is mediated by the newly identified GBA motif.

First, we asked whether GBAS-1 and GOA-1 are expressed in the same cells of living *C. elegans* worms. GOA-1 is one of the best studied Gα proteins in *C. elegans* and its regulation by different types of G protein regulators such as GAPs (e.g., RGS-7), GDIs (e.g., GPR-1/2, AGS-3), or nonreceptor GEFs (e.g., RIC-8) is well characterized (Hajdu-Cronin et al. 1999; Gotta et al. 2003; Afshar et al. 2004; Hess et al. 2004; Hofler and Koelle 2011). Much like its closest homolog in mammals, Gαo, GOA-1 is expressed predominantly in the nervous system (Mendel et al. 1995; Segalat et al. 1995), where it regulates different aspects of neurotransmission, including the neural circuit controlling the egg laying behavior. GOA-1 is also expressed in other cells and plays additional physiological roles (Mendel et al. 1995; Segalat et al. 1995). Most notably, GOA-1 participates in early embryonic development by controlling cell division in coordination with RGS-7, GPR-1/2, and RIC-8 (Gotta et al. 2003; Afshar et al. 2004; Hess et al. 2004). Because the expression pattern of GOA-1 in *C. elegans* tissues is very well documented (Mendel et al. 1995; Segalat et al. 1995), we generated transgenic *C. elegans* strains bearing a green fluorescence protein (GFP) reporter under the control of the GBAS-1 promoter ($P_{gbas\text{-}1}$::GFP) to elucidate the expression pattern of GBAS-1. Previous studies have shown that GOA-1 is expressed in virtually all neurons, distal tip cells (DTC), and some other cells (Mendel et al. 1995; Segalat et al. 1995). In our $P_{gbas\text{-}1}$::GFP transgenic animals we observed GFP signals (fig. 3) in some neurons (head and tail neurons [Neu], HSN, and VC), a subset of glial cells (GLR), distal tip cells (DTC) and intestine. For comparison, we also analyzed the expression of a GFP::GOA-1 reporter (fig. 3*D*). Although the wide expression of GOA-1 in virtually all neurons makes it difficult to visualize single cells in microscopy images, coexpression of a pan-neuronal nuclear RFP marker allowed to pinpoint some of the GOA-1 positive cells, including the HSN neuron that controls egg laying in which $P_{gbas\text{-}1}$::GFP reporter is clearly expressed (fig. 3B). Taken together, these results indicate that GBAS-1 and GOA-1 expressions overlap in many *C. elegans* cells.

Next, we investigated whether GBAS-1 binds directly to GOA-1 by using protein–protein binding assays with purified proteins. Our initial efforts to purify full-length GBAS-1 from *Escherichiacoli* yielded no soluble protein, whereas the C-terminal region of the protein (aa631–758, containing the GBA motif) gave good quantities of high-quality protein when expressed as either His-tagged or GST-tagged fusion protein (supplementary fig. S2, Supplementary Material online). This C-terminal region is separated from the rest of the protein by a predicted intrinsically disordered region (supplementary fig. S2, Supplementary Material online), which indicates that it can work as an independent functional unit and that truncating the protein at aa631 should not disrupt folding of the C-terminal region. We found that GST-fused GBAS-1 binds purified His-GOA-1 when the G protein is in its inactive conformation (i.e., GDP-bound)

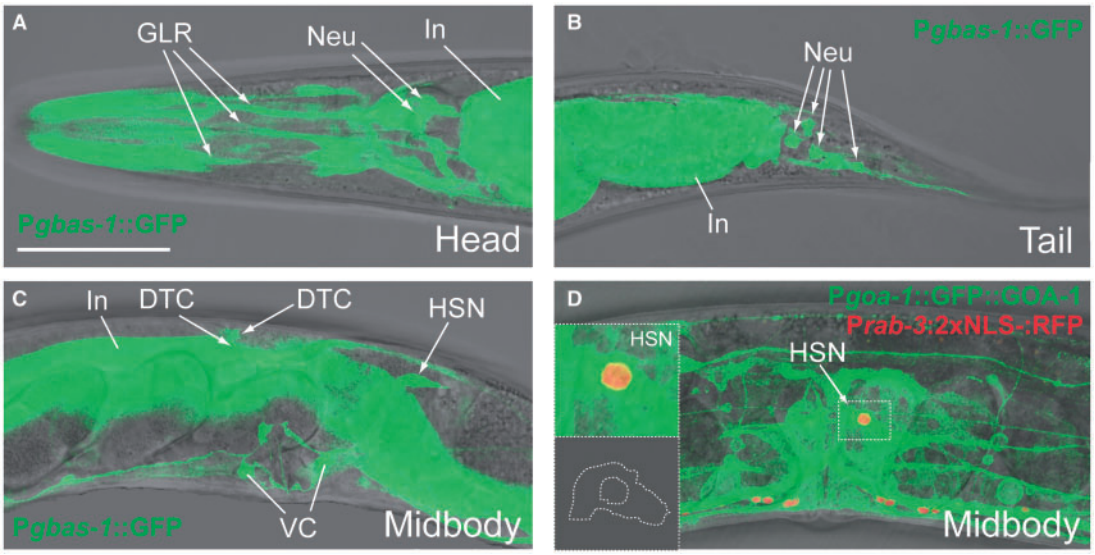

Fig. 3. The expression pattern of *gbas-1* in *Caenorhabditis elegans*. Left: Lateral views of the head (*A*), midbody (*B*), and tail (*C*) of an adult hermaphrodite expressing the P_{gbas-1}::GFP reporter transgene and the midbody (*D*) of an adult expressing a P_{goa-1}::GOA-1::GFP reporter transgene and the pan-neuronal nuclear RFP reporter [P_{rab-3}::2xNLS::TagRFP]. The *gbas-1* reporter is expressed in the head neurons (Neu), glial cells (GLR), and intestine (In) (*A*). It is also expressed in the HSN neuron, DTC, VC neurons (*B*), and tail neurons (*C*). A view of the midbody of an animal expressing the P_{goa-1}::GOA-1::GFP displaying wide expression across neurons is shown for reference. The RFP pan-neuronal reporter is shown to distinguish the localization of the GOA-1::GFP expression in the HSN. Anterior of the animal is to the left, and ventral is down. Scale bar: 50 μm.

(fig. 4A). On the other hand, GBAS-1 binding to active GOA-1, generated by loading with the GTP mimetics GDP-AlF_4^- or GTPγS (Coleman, Berghuis, et al. 1994; Coleman, Lee, et al. 1994; Kleuss et al. 1994), was not detectable (fig. 4A). The preferential binding of GBAS-1 for inactive versus active Gα is a feature shared with other GEFs (Cismowski et al. 2000; Tall et al. 2003; Lee and Dohlman 2008), including all previously characterized GBA proteins and peptides (Johnston et al. 2005; Austin et al. 2008; Ghosh et al. 2008; Garcia-Marcos, Kietrsunthorn, et al. 2011; Aznar et al. 2015). The physiological purpose of binding to inactive but not active G proteins is to ensure the directionality of the reaction toward signaling activation, that is, GEFs bind to inactive G proteins, accelerate the exchange of GDP for GTP, and dissociate upon GTP loading on Gα to allow the action of Gα-GTP on its effectors (Sprang 1997). We estimated the equilibrium dissociation constant (Kd) for the interaction of GBAS-1 with GDP-bound GOA-1 to be approximately 3 μM (fig. 4B and C). This affinity is similar to that of other proteins that regulate Gα in cells (Natochin et al. 2001; Tall et al. 2003; McCudden et al. 2005), including GBA proteins (Garcia-Marcos, Kietrsunthorn, et al. 2011; Aznar et al. 2015), which suggests that the interaction of GBAS-1 with GOA-1 occurs under physiological conditions. Taken together, these results demonstrate that GBAS-1 is present in GOA-1-expressing cells in vivo and that it directly binds to the inactive G protein at physiological concentrations in vitro.

GBAS-1 Binds to GOA-1 through Its GBA Motif

We hypothesized that the putative GBA motif of GBAS-1 was responsible for GOA-1 binding. To gain further insights into how GBAS-1 binds to GOA-1, we generated a homology-based structure model of its GBA motif bound to GOA-1. The model was built using protein–protein docking and the previously resolved structure of human Gαi1 in complex with the GBA-related peptide KB-752 (Johnston et al. 2005). Based on this model, the GBA motif of GBAS-1 docks onto a groove formed between the α3 helix and the Switch II (SwII) region of GOA-1 (fig. 5A). An analysis of the contributions of individual residues to the energetics of the modeled interaction revealed that binding is predominantly stabilized by interactions of hydrophobic nature between residues on one side of an α-helix formed by the GBA sequence and the α3/SwII pocket on Gα (fig. 5A and B). This predicted binding mode is analogous to that of other GBA proteins, which explains the preferential binding to inactive G proteins. This is because the SwII is a structural element that changes conformation depending on whether Gα is bound to GDP or GTP (Sprang 1997). In GDP-bound Gα, the SwII is relatively flexible and can accommodate the GBA motif whereas in GTP-bound Gα, the SwII forms a well-ordered α-helix that shifts to the proximity of the α3 helix and occludes the GBA binding pocket (Sprang 1997).

We reasoned that, if our structural model is correct, GBAS-1 and the KB-752 peptide would compete for binding to GOA-1. We found that this is the case because incubation with the KB-752 peptide inhibited GOA-1 binding to GBAS-1 in a dose-dependent manner (fig. 5C). Although from this single experiment we cannot completely rule out that the KB-752 inhibits the GBAS-1/GOA-1 interaction by binding to GBAS-1, the structural similarity between GOA-1 and Gαi1 indicates that KB-752 inhibits the interaction through a binding to GOA-1. This also suggests that GBAS-1 binds to the α3/SwII pocket of GOA-1 through its GBA motif. To further substantiate this and validate our structural model, we analyzed the contribution of individual residues to the interaction

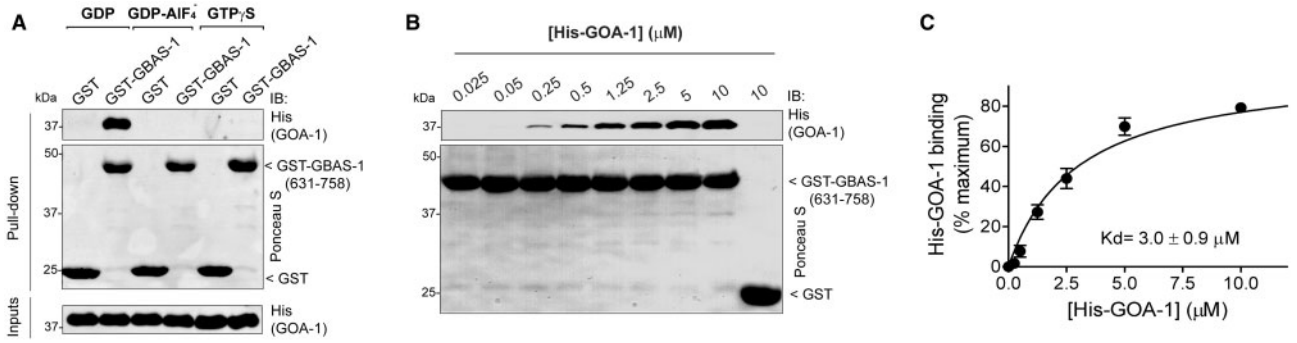

FIG. 4. GBAS-1 binds to the nematode Gα-subunit GOA-1. (*A*) GBAS-1 binds directly to inactive but not to active GOA-1. Twenty micrograms of purified GST-GBAS-1 (aa 631–758, containing the GBA motif) immobilized on glutathione-agarose beads were incubated with 5 μg of purified His-GOA-1 preloaded with GDP (inactive), GDP + AlF_4^- (active) or GTPγS (active) as indicated. Resin-bound proteins were eluted, separated by SDS-PAGE, and analyzed by Ponceau S-staining and immunoblotting (IB) with the indicated antibodies. (*B*, *C*) GBAS-1 binds to inactive GOA-1 with micromolar affinity. Purified GST-GBAS-1 (631–758) immobilized on glutathione-agarose beads was incubated with increasing amounts (0.25–10 μM) of GDP-loaded His-GOA-1 and binding analyzed by immunoblotting. GOA-1 binding was quantified by measuring band intensities and data fitted to a single-site binding hyperbola to calculate the Kd (3.0 ± 0.9 μM). Mean ± S.E.M. of four independent experiments.

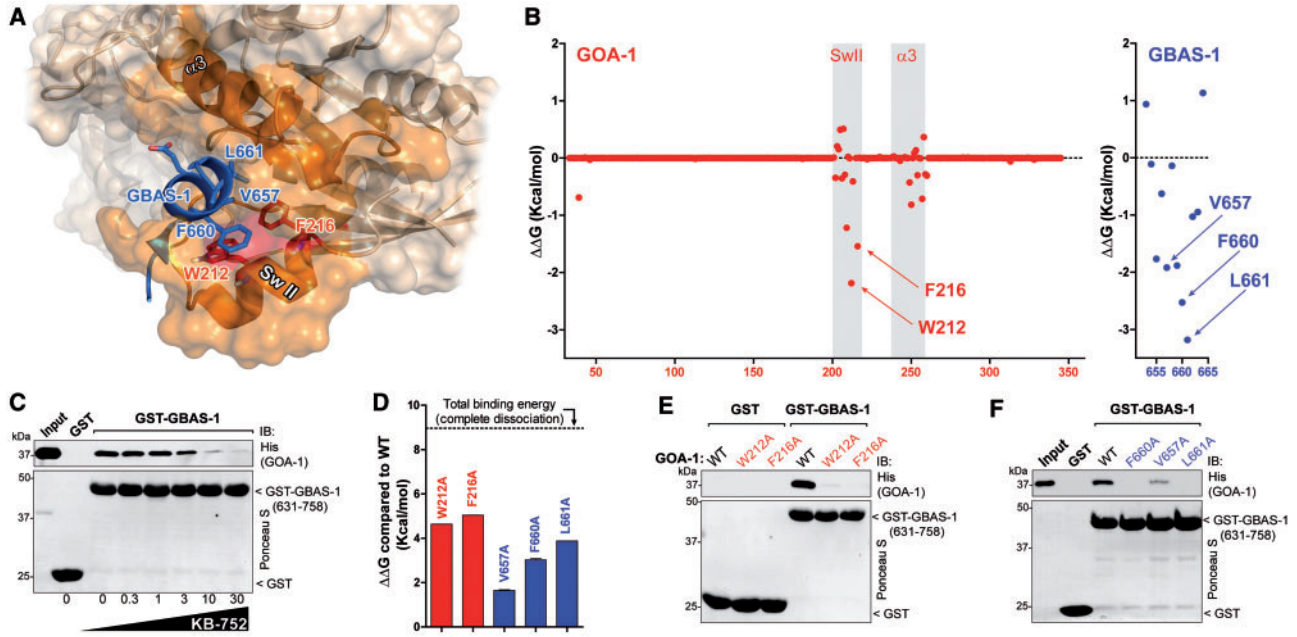

FIG. 5. Characterization of the structural determinants of the GBAS-1/GOA-1 protein interface. (*A*, *B*) Prediction of molecular contacts critical for the GBAS-1/GOA-1 interaction. A homology-based model of GBAS-1 GBA motif (blue) bound to GOA-1 (beige) was generated (*A*) as described in Materials and Methods. Predicted per-residue energy (ΔΔG, kcal/mol) contributions to the total energy of the GOA-1:GBAS-1 complex for the G protein (*B*, left in red) and GBA motif (*B*, right in blue) sides were computationally determined by obtaining the difference in energies of the monomeric components from the binary complex. GBAS-1 (blue) is predicted to engage a hydrophobic cleft formed between SwII and the α3 helix of the GOA-1 (orange). The hydrophobic interaction is predicted to be stabilized primarily by molecular contacts between three hydrophobic residues of GBAS-1's GBA motif (V657, F660, and L661, blue) that line up on one side of an amphipathic helix and two aromatic residues in SwII of GOA-1 (W212, F216, red). (*C*) KB-752 peptide inhibits GBAS-1 binding to GOA-1. Purified GST-GBAS-1 (631–758) immobilized on glutathione-agarose beads was incubated with 5 μg (~0.7 μM) of purified His-GOA-1 in the presence of increasing amounts (0–30 μM) of KB-752, a synthetic peptide known to bind on the cleft between the α3 helix and the SwII region of Gα subunits (Johnston et al. 2005). The results were analyzed exactly as described in figure 4A. One experiment representative of 3 is shown. (*D*) In silico predictions of the effects of interface residue mutations on the total stability of GOA-1:GBAS-1 complex. The effect of individual mutations on the total energy of the GOA-1:GBAS-1 complex was determined by obtaining the difference in energies between the mutant and wild-type complexes (ΔΔG, kcal/mol). The dotted line represents the total energy of the interaction, which would be equivalent to the ΔΔG of a fully dissociated complex. Average ± S.E.M. of five simulations per mutant. (*E*) Mutation of residues in the SwII region of GOA-1 disrupts GBAS-1 binding. Binding of His-GOA-1 WT, W212A or F216A to GST-GBAS-1 (631–758) was analyzed exactly as described in figure 4A. One experiment representative of 3 is shown. (*F*) Mutation of V657, F660, or L661 in the GBA motif of GBAS-1 to alanine disrupts GOA-1 binding. Binding of His-GOA-1 to GST-GBAS-1 (631–758) WT, V657A, F660A, or L661A was analyzed exactly as described in figure 4A. One experiment representative of 3 is shown.

between GBAS-1 and GOA-1 using in silico predictions followed by biochemical validation with site-directed mutagenesis. The analysis of our structural model predicts that V657, F660, and L661 of GBAS-1 and W212 and F216 of GOA-1 are the residues that contribute the most to stabilizing the interaction (fig. 5*A* and *B*). We modeled in silico the mutation of each one of these residues to alanine and evaluated computationally their impact on the energetics of the GBAS-1/GOA-1 interaction (fig. 5*D*). We found that each one of the alanine mutants increases the energy of the complex, indicating impaired binding stability (fig. 5*D*), whereas analogous alanine mutations adjacent to the predicted binding pocket did not affect significantly the energetics of the system ($\Delta\Delta G$ were 0.2, 0.25 and 0.26 kcal/mol for T261A, D262A and K210A, respectively). Next we validated these computational predictions experimentally by carrying out protein–protein binding assays. As predicted, we found that the GOA-1 W212A and F216A mutants had impaired binding to GBAS-1 (fig. 5*E*) and, vice versa, that GBAS-1 mutants V657A, F660A and L661A displayed diminished GOA-1 binding (fig. 5*F*). Taken together, these results demonstrate that GBAS-1 binds to GOA-1 through its GBA motif and that the binding mode of this interaction closely resembles that shown for other GBA motifs in different species.

GBAS-1 Is a *Bona Fide* GEF for GOA-1 *In Vitro*

A GEF is defined by its ability to accelerate the rate of nucleotide exchange. Next, we determined whether the functional consequence of GBAS-1 binding to GOA-1 is the acceleration of nucleotide exchange by performing two well-established enzymatic assays for this purpose—steady-state GTPase and GTPγS binding assays (Krumins and Gilman 2002; Mukhopadhyay and Ross 2002). The former measures the rate of nucleotide exchange indirectly (because GTP hydrolysis is very fast and nucleotide exchange rate limiting under steady-state conditions), whereas the latter measures it directly (Mukhopadhyay and Ross 2002; Afshar et al. 2004). We found that GBAS-1 increases the initial rate of steady-state GTPase activity and GTPγS binding of GOA-1 by approximately 4- to 5-fold (fig. 6*A* and *C*). This extent of GOA-1 activation is comparable to that reported under almost identical experimental conditions for RIC-8, the only other nonreceptor GEF for GOA-1 reported to date (Afshar et al. 2004; Hess et al. 2004; Afshar et al. 2005). GOA-1 activation by GBAS-1 was dose-dependent (fig. 6*B* and *D*) and the EC_{50} values (~3–5 μM) were in keeping with the estimated Kd for the interaction (fig. 4). Importantly, the ability of GBAS-1 to activate GOA-1 was greatly diminished in both assay formats with the GBA mutant F660A (fig. 6*B* and *D*). These results indicate that GBAS-1 is a bona fide GEF for GOA-1 in vitro and that this activity is directly associated with its GBA motif.

GBAS-1 Binds and Activates Mammalian Gαi3

The results shown so far indicate not only that the GBA motif of GBAS-1 shares sequence similarity with GBA motifs in mammalian proteins but also that the GBA–G protein interaction has similar biochemical and structural properties. We reasoned that if G protein activation by GBA proteins is a conserved signaling mechanism, the structure of the GBA/G protein interface would be conserved even among evolutionarily distant species and unrelated proteins. For these reasons, we next asked whether GBAS-1 could bind to mammalian Gα subunits. GOA-1 is the only clear member of the Gi/o family of Gα proteins in *C. elegans* (Bastiani and Mendel 2006), which in mammals diversified into four related proteins: Gαi1, 2, 3, and Gαo. The closest mammalian ortholog of GOA-1 is Gαo (Mendel et al. 1995; Segalat et al. 1995). Yet, all mammalian GBA proteins described to date bind to Gαi subunits (Gαi1, 2, and 3) instead of to Gαo (Johnston et al. 2005; Austin et al. 2008; Garcia-Marcos et al. 2009, 2010; Garcia-Marcos, Kietrsunthorn, et al. 2011; Aznar et al. 2015). Interestingly, we found that GBAS-1 binds and activates mammalian Gα proteins with a marked preference for Gαi3 over Gαo (fig. 7*A* and *C*). In fact, GBAS-1 coupled to Gαi3 as efficiently as to GOA-1. We checked whether the converse is also true, that is, that mammalian GBA proteins can bind to G proteins of *C. elegans*. For testing this, we chose NUCB2 as the mammalian counterpart because its GBA sequence and affinity for Gα are the closest to those of GBAS-1 (Garcia-Marcos, Kietrsunthorn, et al. 2011). Consistent with previous findings (Garcia-Marcos, Kietrsunthorn, et al. 2011), NUCB2 bound preferentially mammalian Gαi3 over Gαo (fig. 7*B*). Moreover, NUCB2 bound GOA-1 as efficiently as Gαi3 (fig. 7*B*), which supports the high conservation of the GBA–G protein binding mode across different species. Of note, although worm GPA-7 is distantly related to mammalian Gαi, a previous report showed that neither GPA-7 nor other worm Gα subunits interact with GBAS-1 in yeast two-hybrid assays (Cuppen et al. 2003), indicating GOA-1 specificity for GBA-mediated regulation. Taken together, these results suggest that the regulation of Gαo-like GOA-1 by a GBA motif in worms was preserved in Gαi and lost in Gαo when the Gi/o family diversified in mammalian cells.

To further validate the conservation of the binding mode between GBAS-1 and Gα subunits of different species, we tested the effect of the GBA mutant F660A that precludes binding and activation of GOA-1 (figs. 5 and 6). We found that the F660A mutation decreased GBAS-1-mediated activation of mammalian Gαi3 as efficiently as it does for GOA-1 (fig. 7*C*), indicating that GBAS-1 activates both G proteins by using an analogous GBA motif-dependent mechanism. Next, we tested whether GBAS-1 activates Gαi3 also in cells by taking advantage of a previously validated yeast-based assay (Cismowski et al. 1999, 2002). Briefly, we introduced GBAS-1 WT and F660A in a genetically engineered yeast strain that lacks GPCRs and with the endogenous yeast Gα protein GPA1 replaced by mammalian Gαi3 (fig. 7*D*). In this system, only an exogenous G protein activator can trigger a signaling pathway that is normally activated as a pheromone response leading to an increase in Fus3 phosphorylation and in transcriptional activation of the Fus1 gene (fig. 7*D*). We also introduced in this strain the nonreceptor GEF Ric-8A to compare activation efficiency with GBAS-1. Ric8 proteins are well-characterized nonreceptor GEFs and the only ones known to date that activate both *C. elegans* GOA-1 and mammalian Gα

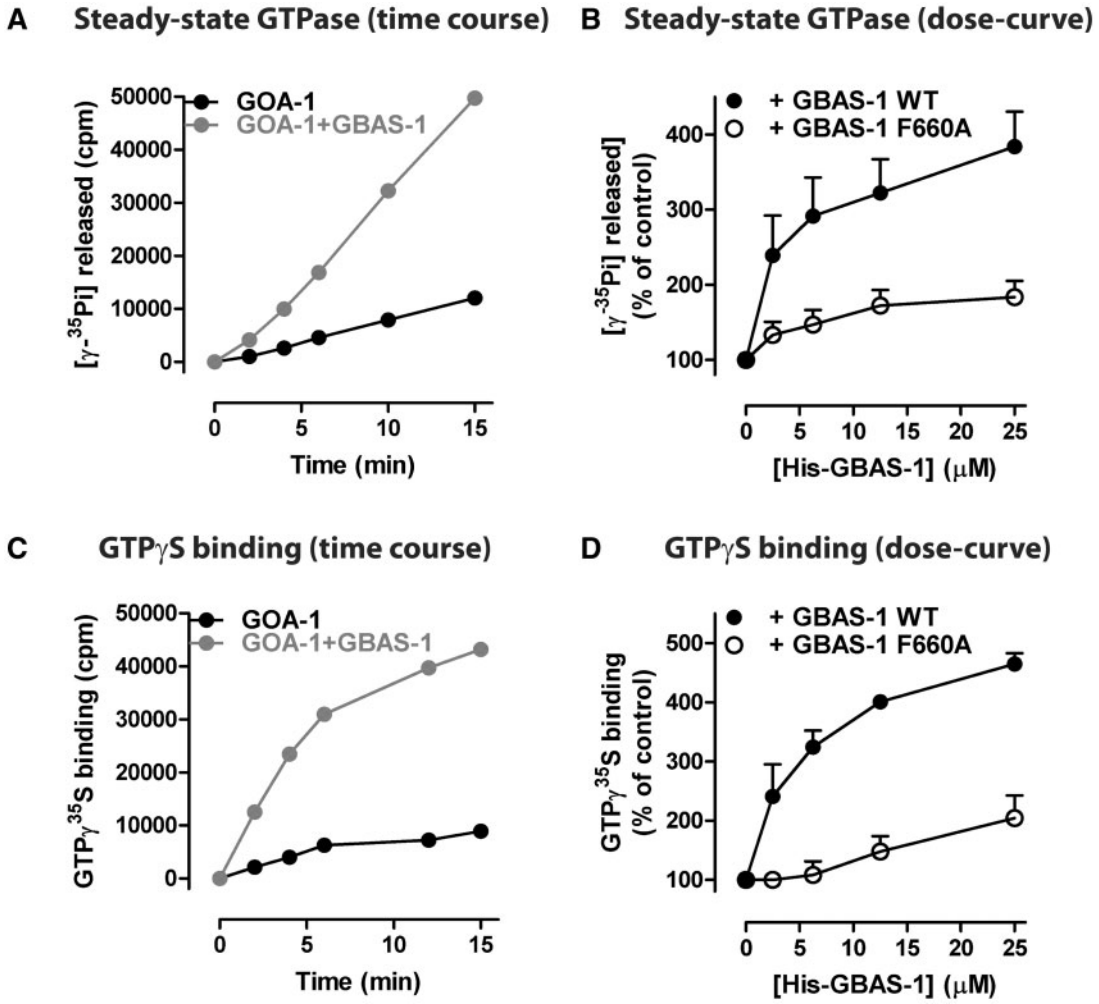

Fig. 6. GBAS-1 is a bona fide GEF for GOA-1. (*A*) GBAS-1 accelerates the rate of GOA-1 steady-state GTPase activity. The steady-state GTPase activity of His-GOA-1 alone (black) or in the presence of 25 μM His-GBAS-1 (aa631–758, gray) was determined by measuring the production of [^{32}P]Pi at different time points as described in Materials and Methods. One experiment representative of 3 is shown. (*B*) GBAS-1 WT but not F660A accelerates the rate of GOA-1 steady-state GTPase activity in a dose-dependent manner. The steady-state GTPase activity of His-GOA-1 was determined in the presence of increasing concentrations (0–25 μM) of His-GBAS-1 WT (closed circles) or His-GBAS-1 F660A (open circles) by measuring the production of [^{32}P]Pi at 15 min. Mean ± S.E.M. of five independent experiments. The EC_{50} (5.14 ± 2.25 μM) for GBAS-1 WT was calculated by fitting the data to a sigmoidal dose–response curve. (*C*) GBAS-1 accelerates the initial rate of GTPγS binding to GOA-1. GTPγ^{35}S binding to His-GOA-1 alone (black) or in the presence of 25 μM His-GBAS-1 (aa631–758, gray) was determined as described in Materials and Methods. One experiment representative of 3 is shown. (*D*) GBAS-1 WT but not GBAS-1 F660A dose-dependently accelerates the rate of GTPγS binding to GOA-1. GTPγ^{35}S binding to His-GOA-1 at 15 min was determined in the presence of increasing concentrations (0–25 μM) of His-GBAS-1 WT (closed circles) or His-GBAS-1 F660A (open circles). Mean ± S.E.M. of four independent experiments. The EC_{50} (3.14 ± 1.89 μM) for GBAS-1 WT was calculated by fitting the data to a sigmoidal dose–response curve.

proteins (including Gαi) in vitro and in vivo (Tall et al. 2003; Afshar et al. 2004; Hess et al. 2004; Papasergi et al. 2015). We found that GBAS-1 WT but not the GEF-deficient mutant F660A enhances Gαi3-dependent signaling in cells as determined by increased Fus3 phosphorylation (fig. 7*E*) and P_{Fus1}::LacZ reporter activity (fig. 7*F*). The extent of the activation by GBAS-1 WT was similar to that observed for Ric-8A in both assays (fig. 7*E* and *F*). Taken together, these results indicate that GBAS-1 can activate Gα subunits of a different species in vitro and in cells. This activation occurs through a conserved molecular mechanism that requires the GBAS-1 GBA motif and is as efficient as previously validated nonreceptor GEFs.

Structural Basis for GBAS-1 Preference for Gαi3 and GOA-1 versus Gαo

The preference of GBAS-1 for mammalian Gαi3 versus Gαo is somewhat puzzling because its substrate G protein in *C. elegans*, GOA-1 (*G protein, o, alpha subunit*), has higher similarity to mammalian Gαo than to Gαi3. We reasoned that specific differences in the structural features of the GBA binding region of Gα proteins would be responsible for the preferential binding of GBAS-1 to GOA-1 and Gαi3 over Gαo. We aligned the protein sequences corresponding to the GBA binding region of GOA-1, Gαi3, and Gαo (fig. 8*A*) and found that, despite all being similar, GOA-1 resembled Gαi3 more closely than Gαo. To gain further insights into how

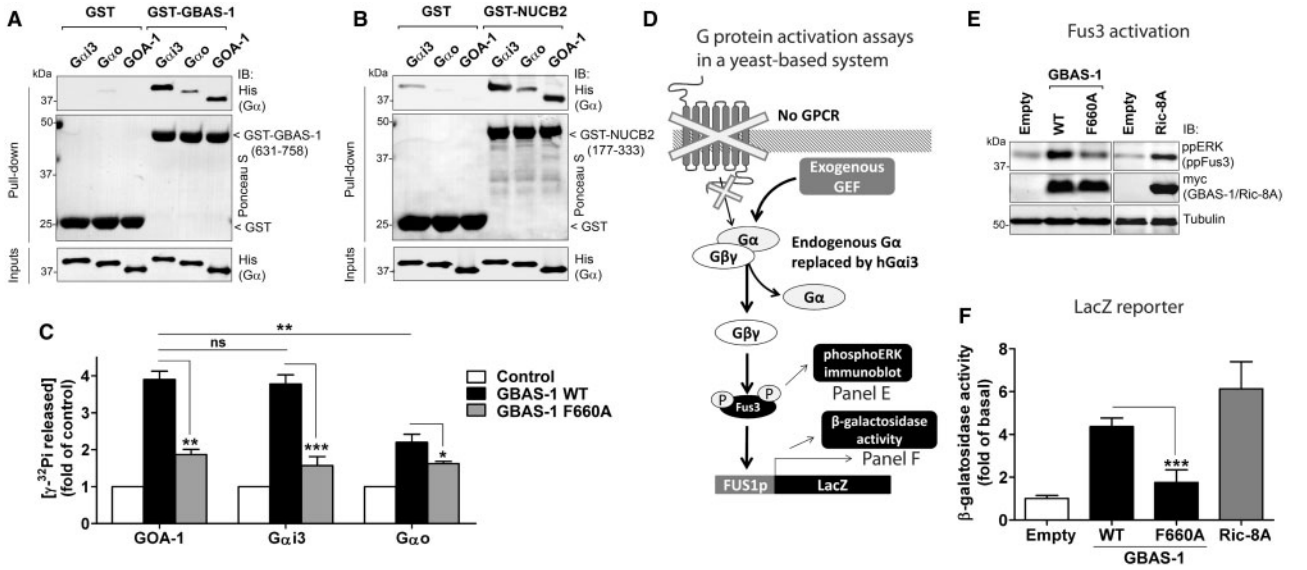

Fig. 7. GBAS-1 binds and activates mammalian Gαi3 more efficiently than mammalian Gαo. (*A*) GBAS-1 binds to mammalian Gαi3 as efficiently as to GOA-1 and better than to mammalian Gαo. Binding of His-GOA-1, His-Gαi3, or His-Gαo to GST-GBAS-1 (631–758) was analyzed exactly as described in figure 4*A*. (*B*) NUCB2, a mammalian GBA protein, binds to GOA-1 as efficiently as to mammalian Gαi3 and better than to mammalian Gαo. Binding of His-GOA-1, His-Gαi3, or His-Gαo to GST-NUCB2 (aa177–333, containing the GBA motif) was analyzed exactly as described in figure 4*A*. (*C*) GBAS-1 activates mammalian Gαi3 through its GBA motif as efficiently as *Caenorhabditis elegans* GOA-1 and better than mammalian Gαo. The steady-state GTPase activity of His-GOA-1, His-Gαi3, or His-Gαo was determined in the presence of 25 μM His-GBAS-1 WT (black bars) or His-GBAS-1 F660A (gray bars) by measuring the production of [^{32}P]Pi at 15 min. results are expressed as fold activation compared with the G protein alone (white bars). Mean ± S.E.M. of 4–8 independent experiments. $^{*}P < 0.05$, $^{**}P < 0.01$, $^{***}P < 0.001$. (*D*) Schematic diagram of yeast-based assays to monitor G protein activation by GBAS-1. The pheromone response pathway in *Saccharomyces cerevisiae* is regulated by GPCR-mediated activation of trimeric G proteins, which induces Fus3 phosphorylation and transcriptional activation of the Fus1 promoter. A genetically engineered strain lacking endogenous GPCRs, with a mammalian Gαi3 replacing the endogenous Gα GPA1 and bearing a LacZ reporter under the control of the Fus1 promoter was used to determine the levels of G protein activation upon expression of exogenous GEFs like GBAS-1 or Ric-8A. Fus3 activation was determined by phosphoERK (ppERK, which recognizes yeast ppFus3) immunoblotting (panel *E*) and β-galactosidase activity assays (panel *F*). (*E*) GBAS-1 WT but not GBAS-1 F660A enhances Fus3 activation in yeast as efficiently as Ric-8A. Yeast cells expressing GBAS-1 WT (aa631–758), GBAS-1 F660A, Ric-8A (aa12–491), or an empty vector were lysed and proteins analyzed by immunoblotting with the indicated antibodies as described in Materials and Methods. One representative strain out of at least 3 is shown. (*F*) GBAS-1 WT but not GBAS-1 F660A enhances the Fus1 transcriptional activity in yeast as efficiently as Ric-8A. The β-galactosidase activity of yeast cells expressing GBAS-1 WT (aa631–758), GBAS-1 F660A, Ric-8A (aa12–491), or an empty vector was measures as described in Materials and Methods. Mean ± S.E.M. of at least three independent strains. $^{***}P < 0.001$.

the higher similarity of GOA-1 to Gαi3 may contribute to favor the interaction with GBAS-1, we modeled the three-dimensional structure of the GBA binding site of GOA-1 on Gαi3 and Gαo (fig. 8*B–D*). When we mapped sequence similarity to GOA-1 on the predicted GBA binding surfaces of Gαi3 and Gαo, we found that that the amino acid composition of the GBA binding surface on Gαi3 was identical to GOA-1 whereas it differed in two residues for Gαo (fig. 8*C* and *D*, same amino acid as in GOA-1 are in red, different in green). These two residues in Gαo are M249 and F259, which correspond to K249 and W259 in GOA-1 and K248 and W258 in Gαi3. This suggests that the presence of K249 and/or W259 in GOA-1 is important to favor its binding to GBAS-1 and that their mutation to the corresponding amino acid(s) in Gαo would have a deleterious effect on the interaction. We tested separately each one of these mutants for binding to GBAS-1 and found that GOA-1 K249M reduced binding whereas W259F had no effect (fig. 8*E*). These results indicate that, despite the overall similarity between GOA-1 and Gαo, the GBAS-1 binding site on GOA-1 has structural features that closely resemble the GBA binding site of Gαi in mammalian proteins. This indicates that the structural features of the GBA–G protein interface are highly conserved in distant species even in the context of different Gα subtypes, suggesting that this binding mode is preserved by selective pressure.

Final Remarks and Future Perspectives

The main finding of this work is the identification of a nonreceptor GEF of the GBA family in invertebrates. This indicates that the mechanism of receptor-independent activation of trimeric G proteins by GBA proteins appeared at least 300 Ma. Importantly, the newly identified GEF, GBAS-1, is found only in *C. elegans* and is not related to any of the previously characterized GBA proteins other than by the presence of the GEF motif. Despite the overall divergence between GBAS-1 and mammalian GEFs, the GBA motif of GBAS-1 is capable of activating mammalian G proteins. These findings demonstrate that the GBA motif is a functional GEF module conserved in evolutionarily divergent proteins and suggest that its function is preserved due to selective pressure. We provide evidence that the functional conservation of the GBA motif as

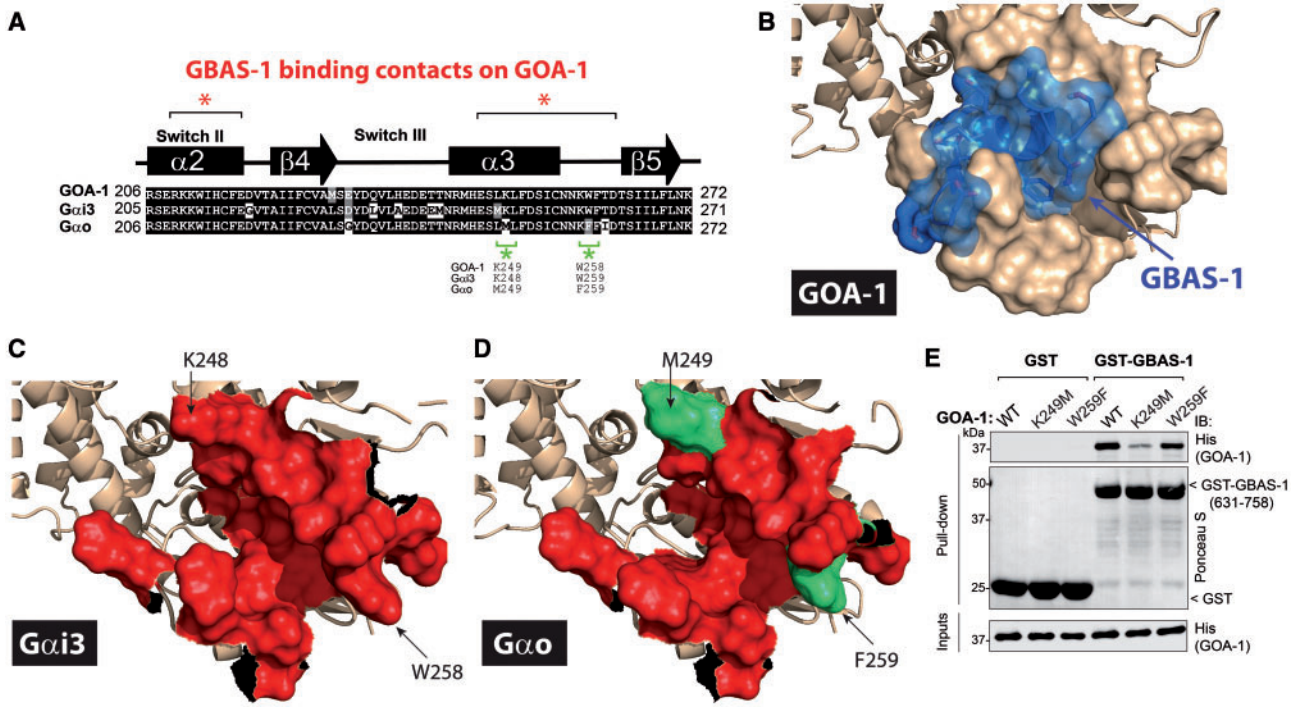

FIG. 8. Structural basis for GBAS-1 coupling to different Gα subunits in vertebrates and invertebrates. (*A*) Alignment of the GBA-binding region in GOA-1, rat Gαi3, and rat Gαo. Protein sequences were aligned using ClustalW. Black and gray shading indicate conservation of identical or similar residues. (*B–D*) Comparative analysis of the GBAS-1 binding site on GOA-1, Gαi3, and Gαo. Homology-based models (beige) of GOA-1 (*B*), Gαi3 (*C*), and Gαo (*D*) in GBAS-1-bound conformations are shown in the same orientation to compare the structural features of the binding interface. GBAS-1 (blue) is not shown in the Gαi3 and Gαo models for clarity. Red surface overlay indicates residues conserved with GOA-1 whereas green indicates sequence deviation. (*E*) Mutation of K249 to M in GOA-1 impairs its binding to GBAS-1 whereas mutation of W259 to F has no effect. Binding of His-GOA-1 WT, K249M or W259F to GST-GBAS-1 (631–758) was analyzed exactly as described in figure 4.

a GEF for G proteins of distant species arises from constrains in the GBA-Gα binding mode at the structural level. This is because, in addition to the sequence similarity of the GBA motif in GBAS-1 and other mammalian GBAs, the binding site on Gα is essentially identical in different species (fig. 8) and highly sensitive to subtle single residue variations (e.g., replacement of K249 in GOA-1 by methionine).

The lack of GBAS-1 orthologs out of the *Caenorhabditis* genus and its unrelatedness to previously described GBA proteins (except for its GEF motif) are features remarkably similar to those of another G protein regulator of *C. elegans*, GPR-1. GPR-1, and the very close paralog GPR-2, contains a GoLoco GDI motif (Gotta et al. 2003). Much like in the case of GBAS-1, there are GPR-1/2 orthologs only in the *Caenorhabditis* genus and their similarity to other GoLoco motif-containing proteins in metazoans is restricted to the GDI motif (Hofler and Koelle 2011). These observations are interesting because they suggest similar evolutionary mechanisms for the appearance and conservation of G protein regulatory modules of different kinds (GBA vs. GoLoco).

A question that remains open is about the physiological function of GBAS-1 as a G protein regulator. The general function of GBAS-1 is unknown and a previous paper reported that its depletion by RNAi causes no overt phenotype in worms (Cuppen et al. 2003). We generated GBAS-1 knockout worm strains and did not observe any major phenotypic alteration (no lethality, sterility or major locomotor defects). We also analyzed in detail egg-laying behavior, which is regulated by GOA-1 expressed in HSN neurons (Mendel et al. 1995; Tanis et al. 2008). Because GBAS-1 is also expressed in HSN neurons (fig. 3), we reasoned that it could specifically affect egg-laying behavior. GOA-1 regulates different aspects of egg-laying behavior depending on the environmental conditions. For example, it regulates normal egg laying under standard culture conditions (well fed) but it is also responsible for shutting down egg-laying under starved conditions and for resuming egg-laying after refeeding. Because different GOA-1 regulators have been shown to regulate egg-laying at different steps of this fed-starved cycle (Dong et al. 2000; Hofler and Koelle 2011), we tested the behavior of GBAS-1 knockout animals in three different conditions, fed, starved and refed (Supplementary fig. S3*A*, Supplementary Material online). We found that GBAS-1 knockout animals have no major alterations in egg-laying behavior because they lay eggs efficiently under fed conditions, shut off egg laying under starvation, and resume egg-laying upon refeeding (Supplementary fig. S3*A*, Supplementary Material online). We noticed a modest decrease in the number of eggs laid by GBAS-1 under fed and refed conditions. We reasoned that if this defect is due to reduced egg-laying activity, the number of unlaid eggs in the GBAS-1 knockout worms would be increased. However, we found that this is not the case. Instead, the number of unlaid eggs is slightly decreased compared with wild-type animals (Supplementary fig. S3*B*,

Supplementary Material online). These results indicate that the diminished number of laid eggs is likely a consequence of diminished egg production rather than an effect on egg-laying per se. Although egg production is known to be regulated by GOA-1 (Mendel et al. 1995; Segalat et al. 1995), the defect observed in GBAS-1 knockout animals is too mild to know with certainty if it is biologically relevant and/or related to GOA-1. Thus, although these results suggest an in vivo role for GBAS-1, establishing its specific function as a G protein regulator will require additional work. For example, it is possible that functional redundancy with other proteins with an uncharacterized GBA function in *C. elegans* (like some of the hits shown in fig. 2) may account for the lack of phenotype alterations upon GBAS-1 deletion. Another possibility is that GBAS-1 regulates GOA-1 for physiological functions in which GOA-1 activity is redundant with other Gα subunits. Previously published (Cuppen et al. 2003) yeast two-hybrid data suggest that GBAS-1 is specific for GOA-1, so it is possible that the functional redundancy of different Gα would mask GBAS-1 effects. In fact, functional redundancy of GOA-1 and other Gα subunits is well documented, especially in the context of cell division regulation during early development (Gotta and Ahringer 2001; Afshar et al. 2005). In this context, GOA-1 and GPA-16 have redundant functions and both of them must be simultaneously deleted to observe impaired cell division and cause a severe embryonic lethal phenotype (Gotta and Ahringer 2001). Interestingly, deletion of the nonreceptor GEF RIC-8 also causes severe embryonic lethality and it has been demonstrated that this is due to its ability to simultaneously regulate both GOA-1 and GPA-16 in cell division (Afshar et al. 2005). Reduced egg production is associated with the loss of function of GOA-1 in embryonic cell division (Gotta and Ahringer 2001; Afshar et al. 2004), so it is possible that the mildness of the loss of egg production in GBAS-1 knockout animals (Supplementary fig. S3, Supplementary Material online) is due to GPA-16 functional redundancy. In summary, additional work is required to address the specific function(s) of GOA-1 regulated by GBAS-1 in vivo.

Regardless of the specific physiological function of GBAS-1 in *C. elegans*, our results establish that this protein is a bona fide GEF for Gα in vitro and that it can activate G protein signaling in cells. Because this mechanism was elucidated by searching for a conserved GBA motif, our work also provides the proof-of-principle for the identification of nonreceptor GEFs of the GBA class in different evolutionary lineages based solely on sequence similarity. However, the relatively low number of known GBA sequences is still a limitation to perform powerful searches and the chances of false positives would be too high to allow their systematic identification based only on sequence similarity. For example, we used the same query sequence and program (ScanSite3) as reported here for *C. elegans* to search the proteomes of *D. rerio* and *Mus musculus*. We obtained 19, 33 and 25 hits with scores below the threshold of ScanSite3 (<0.2) in *C. elegans*, *D. rerio* and *M. musculus*, respectively. Although we identified ccdc88 orthologs among the hits in *D. rerio* and *M. musculus*, the rest of the hits were unrelated proteins and it would be a daunting task to validate each one of them separately. Therefore, the validation of additional GEFs of the GBA family in different species, like the one reported here, would be useful to build a more robust training set. Moreover, the validation of additional GBA proteins would also be useful to establish additional parameters to be implemented to filter/refine the results of sequence searches. For example, the GBA motif of GBAS-1 is predicted to be present in an intrinsically disordered region (Supplementary fig. S1, Supplementary Material online), as it occurs with the GBA motif of GIV and DAPLE (Oates et al. 2013). Whether this is a true conserved feature for GBA motifs remains to be established but, if so, it could be used as an additional parameter during candidate identification. Further advances toward defining the GBA sequence conservation and other GBA-associated structural features will be critical for developing more accurate tools for the identification and subclassification of novel nonreceptor GEFs. These efforts would be the next rational step to understand the evolutionary history of this GPCR-independent mechanism of trimeric G protein activation.

Materials and Methods

Bioinformatics Analyses and Searches

Sequences of ccdc88 orthologs were obtained using two complementary approaches. First, we used the database of orthologs OrthoDB (Kriventseva et al. 2008). We retrieved the 157 ccdc88 sequences annotated in Uniprot from Group EOG7N0C3V in this database. These sequences belonged to 67 metazoan species. Second, we used BLASTp to increase the coverage of species in our analysis of ccdc88 orthologs. More specifically, we searched additional invertebrate species to balance the number of vertebrates versus invertebrates (final numbers were 38 vs. 46) and additional nonmetazoan species. The invertebrate species were selected to cover major metazoan groups not well represented in the data set obtained from OrthoDB: Porifera, Ctenophora, Placozoa, Cnidarian, and different subgroups of Bilaterialia. We also searched in five holozoans of three different classes (Coanoflagelata, Filasterea, and Ichthyosporea), nine fungi of six different classes (Ascomycota, Basidiomycota, Mucoromycota, Blastocladiomycota, Chytridiomycota, and Microsporidia), two amoebas and seven bikonts from Excavata, Alveolata, Heterokonta, and Embryophyta. The searches in BLASTp were conducted using three independent ccdc88 sequences against each species. We used ccdc88 proteins from *H. sapiens* (Uniport: Q3V6T2), *Drosophila melanogaster* (Uniprot: Q8SX64), and *C. elegans* (Uniprot: Q9XXR1) to ensure that we did not miss distant relatives. For each search in individual species, we selected the Basic Local Alignment Search Tool (BLAST) hits with lower Expected values (*E* values) among the queries with the three different ccdc88 sequences. Hits with *E* values larger than 10^{-5} were discarded. The total number of sequences was 201, which corresponded to 109 different species (ccdc88 proteins were absent in 19 of these species). Sequences were imported into the Genenious software (Kearse et al. 2012) for

visualization and for searching GBA motifs using the sequence pattern [LIMV]-[TS]-[LIMV]-x-[DEQ]-[F]-[LIMV]. Sequences were manually annotated for the presence of a GBA motif and analyzed for the number of ccdc88 family members per species and how many of them had a GBA motif.

The search for proteins with a GBA motif in *C. elegans* was performed in ScanSite 3 using the QuickMatrix Method (Obenauer et al. 2003). Briefly, we used the sequences of known GBA motifs of the proteins GIV, DAPLE, NUCB1, NUCB2 and the synthetic peptides KB-752 and GSP (Johnston et al. 2005; Austin et al. 2008; Garcia-Marcos et al. 2009; Garcia-Marcos, Kietrsunthorn, et al. 2011; Aznar et al. 2015) to design the pattern [V(L)]-[T]-[L(V)]-[X(E)]-[DE]-[F]-[L] and generate the corresponding PSSM to search in the *C. elegans* proteome in the NCBI Protein GenPept/RefSeq database.

Sequence similarity searches and domain annotations in Pfam and SMART databases for *C. elegans* F59H5.1 (a.k.a. GBAS-1) were performed in BLASTp using default parameters against the nonredundant protein sequences (nr) database. Hits with *E* values $<$1e-6 were considered as GBAS-1-related homologs and searched for the presence of a GBA motif using the sequence pattern [LIMV]-[TS]-[LIMV]-x-[DEQ]-[F]-[LIMV] as described above. Alignment of GBAS-1-related protein amino acid sequences was performed in Geneious v4.8.4 (Biomatters LTD.) with the Blosum62 cost matrix and 99 refinement iterations. Alignments for CBG20133 and CBG11397 were further refined manually to maximize pairwise identity to similar sequences. Phylogenetic analysis was performed using this alignment in MEGA6 (Tamura et al. 2013). The corresponding cladogram was built using the maximum-likelihood method with a Whelan and Goldman substitution model (Whelan and Goldman 2001) inclusive of a frequency parameter and five discrete gamma distribution categories (WAG+Freq.+G). Selection of model was based on comparison of Bayesian Information Criterion scores (lowest chosen). Bootstrap consensus tree (Felsenstein 1985) was inferred from 500 replicates.

Protein secondary structure and disorder predictions were done using PSIPRED v3.3 and DISOPRED3, respectively, using the PSIPRED server (Buchan et al. 2013).

Plasmid Constructs and Mutagenesis

A cDNA of F59H5.1 (a.k.a. GBAS-1) was obtained from OpenBiosystems and used as a template for polymerase chain reaction amplification of the region corresponding to aa631–758. This fragment was cloned into ligation independent cloning (LIC) vectors derived from pET21 (Stols et al. 2002; Cabrita et al. 2006) (kindly provided by John Sondek, University of North Carolina, Chapel Hill) as an N-terminally tagged GST-fused protein or a His-tagged protein using previously described protocols. The plasmid encoding for GST-NUCB2 (177–333) has been described previously (Garcia-Marcos, Kietrsunthorn, et al. 2011). GOA-1 (aa28–351) was cloned into an LIC vector as an N-terminally tagged His-fused protein. This N-terminally truncated GOA-1 has been previously validated to preserve the in vitro biochemical properties of the native protein, including susceptibility to activation by nonreceptor GEFs (Afshar et al. 2004, 2005). The plasmids encoding for rat His-Gαi3 and rat His-Gαo have been described previously (Garcia-Marcos et al. 2010). GBAS-1 (631–758) and rat Ric-8A (aa12–491, kindly provided by Stephen Sprang, University of Montana [Thomas et al. 2011]) were cloned into an LIC vector derived from pYES2. Briefly, this plasmid was created by removing two *Ssp*I sites (nt 5379 and 5400) by mutagenesis and inserting the LIC cassette described in Stols et al. (2002) between the *Ssp*I/*Bam*HI sites of the multicloning site resulting in the elimination of the *Ssp*I site and preservation of the *Bam*HI site. A sequence containing the first 9 aa of *Saccharomyces cerevisiae* GPA1 followed by a myc tag was cloned upstream of the LIC cassette between the *Hin*dIII and *Kpn*I sites. The GBAS-1 and Ric-8A fragments were then inserted using previously described LIC procedures (Stols et al. 2002; Cabrita et al. 2006). The centromeric pRS314 plasmid containing the LacZ gene under the control of the Fus1 promoter was a kind gift of Mary Cismowski (Nationwide Children's Hospital; Cismowski et al. 2002). A transgene to express green fluorescent protein in *C. elegans* from the *gbas-1* promoter was generated by amplifying a 5-kb promoter fragment using the primers 5′-acgtGGATCCcattttgctgaaaattacatttaaag-3′ and 5′-acgtCTGCAGcgtattactttcacaaacctccc-3′ from a fosmid clone containing *gbas-1* genomic DNA, cutting with *Bam*HI and *Pst*I (sites shown in capital letters within the primer sequences), and inserting into the GFP expression vector pPD96.77 (Andrew Fire, Stanford University) also cut with *Bam*HI and *Pst*I. The transgenes to express GFP::GOA-1 from the *goa-1* promoter and the pan-neuronal RFP reporter [*Prab-3::2xNLS::TagRFP*] were described previously (Jose et al. 2007; Stefanakis et al. 2015). Site-directed mutagenesis was carried out using the QuickChange kit (Agilent) following the manufacturer's protocol (primers available upon request).

Caenorhabditis elegans Strains and Microscopy

Caenorhabditis elegans strains were cultured at 20 °C on nematode growth medium (NGM) agar plates with *E. coli* strain OP50 as a food source (Brenner 1974). The wild-type strain was Bristol N2. Two *C. elegans* strains bearing mutant alleles for the *gbas-1* gene were obtained from the International *C. elegans* Gene Knockout Consortium. The two alleles were *gk578844* and *gk136226*, which bear early nonsense mutations (stop codons) replacing K575 and Q337, respectively. These alleles are expected to produce no protein (due to nonsense-mediated decay of the mRNA) or truncated proteins lacking the GBA motif. Each mutant strain was outcrossed at least four times to the wild-type to produce the two *gbas-1* mutant strains analyzed, LX1967 *gbas-1(gk136226)* and LX1968 *gbas-1(gk578843)*. Transgenic strains expressing the $P_{gbas\text{-}1}$::GFP reporter cassette were constructed by injection of plasmid DNA into the germline. LX2147 *vsIs161*[P*goa-1*::GOA-1::GFP]; *otIs356*[P*rab-3*::2xNLS::TagRFP] animals were used to image the GOA-1::GFP (Jose et al. 2007) and the pan-neuronal nuclear RFP marker expression (Stefanakis et al. 2015). Animals were immobilized for microscopy on agar pads with a drop of

0.1% (w:v) levamisole and imaged with a Zeiss LSM 710 confocal microscope.

Caenorhabditis elegans Egg-Laying Assays

Egg-laying assays were performed as previously described (Dong et al. 2000; Chase and Koelle 2004; Hofler and Koelle 2011). To determine the number of unlaid eggs, adult animals were dissolved in bleach and the number of bleach-resistant eggs counted. In the unlaid egg assay, 36 animals per genotype were analyzed. To measure response to starving and feeding, staged adults were picked to an unseeded plate and allowed to crawl away from residual food for 3–5 min, and then repicked to an NGM plate containing OP50 bacteria (fed condition) or a plate containing no food (starved condition). Plates for each condition had a 4 M fructose ring applied as an osmotic barrier approximately 15–20 min before starting the experiment. Animals were allowed to lay eggs for 60 min and were then removed from plates and eggs were counted. The adults removed from the starved condition plates were moved to plates containing food (refed condition) and were allowed to lay eggs for an additional 60 min. They were then removed and the eggs laid were counted. The number of eggs laid was determined by assaying 50 animals per condition for each genotype (five experiments of ten animals each). Adults used for both assays were obtained by picking late L4 larvae and staging the animals for 40 h at 20 °C.

Protein Expression and Purification

GST- and His-tagged recombinant proteins were expressed in *E. coli* strain BL21(DE3) (Invitrogen) and purified as described previously (Garcia-Marcos et al. 2010; Garcia-Marcos, Kietrsunthorn, et al. 2011). Briefly, bacterial cultures were induced overnight at 23 °C with 1 mM isopropyl-β-D-1-thiogalactopyranoside (for His-tagged G proteins) or following an "autoinduction" protocol as described in Studier (2005) (for GST- and His-tagged GBAS-1). Pelleted bacteria from 1 l of culture were resuspended in 25 ml GST-lysis buffer (25 mM Tris–HCl, pH7.5, 20 mM NaCl, 1 mM ethylenediaminetetraacetic acid [EDTA], 20% [v/v] glycerol, 1% [v/v] Triton X-100 supplemented with protease inhibitor cocktail [Leupeptin 1 μM, Pepstatin 2.5 μM, Aprotinin 0.2 μM, PMSF 1 mM]) or in 25 ml His-lysis buffer (50 mM NaH_2PO_4[pH 7.4], 300 mM NaCl, 10 mM imidazole, 1% [v/v]Triton X-100 supplemented with protease inhibitor cocktail [Leupeptin 1 μM, Pepstatin 2.5 μM, Aprotinin 0.2 μM, PMSF 1 mM]) for GST or His-fused proteins, respectively. After sonication (four cycles, with pulses lasting 30 s/cycle, and with 1-min interval between cycles to prevent heating), lysates were centrifuged at 12,000 × g for 20 min at 4 °C. Solubilized proteins were affinity purified on glutathione-agarose beads (Pierce) or HisPur Cobalt Resin (Pierce), eluted with reduced glutathione or imidazole followed by overnight dialysis against phosphate-buffered saline (PBS) and storage at − 80 °C. For the purification of His-GBAS-1, the dialysis step was replaced by a gel filtration chromatographic step in a Superdex S200 column equilibrated with PBS. For the purification of G proteins, buffers were supplemented with 25 μM GDP and proteins exchanged into 20 mM Tris–HCl, pH 7.4, 20 mM NaCl, 1 mM $MgCl_2$, 1 mM dithiothreitol (DTT), 10 μM GDP, and 5% (v/v) glycerol before storage at − 80 °C.

In Vitro Protein Binding Assays

GST pulldown assays were carried out as described previously (Garcia-Marcos et al. 2010; Garcia-Marcos, Kietrsunthorn, et al. 2011) with minor modifications. Briefly, 20–25 μg of GST, GST-GBAS-1 (631–758), or GST-NUCB2 (177–333) were immobilized on glutathione agarose beads for 90 min at room temperature in PBS. Beads were washed twice with PBS, resuspended in binding buffer (50 mM Tris–HCl, pH 7.4, 100 mM NaCl, 0.4% [v:v] NP-40, 10 mM $MgCl_2$, 5 mM EDTA, 2 mM DTT, and 30 μM GDP), and incubated 4 h at 4 °C with constant tumbling in the presence of different His-tagged G proteins. Beads were washed four times with 1 ml of wash buffer (4.3 mM Na_2HPO_4, 1.4 mM KH_2PO_4, pH 7.4, 137 mM NaCl, 2.7 mM KCl, 0.1% [v/v] Tween-20, 10 mM $MgCl_2$, 5 mM EDTA, 1 mM DTT, and 30 μM GDP) and resin-bound proteins eluted with Laemmli sample buffer by incubation at 37 °C for 10 min. Proteins were separated by sodium dodecyl sulfate polyacrylamide gel electrophoresis (SDS-PAGE) and transferred to Polyvinylidene fluoride (PVDF) membranes. After blocking with PBS supplemented with 5% nonfat milk, membranes were analyzed by Ponceau S staining (GST-fused proteins) or sequential incubation with primary and secondary antibodies. Primary anti-His antibodies (Sigma H1029) were used at 1:2,500 dilution and secondary antibodies (Goat antimouse IRDye 800 F(ab′)2, Li-Cor Biosciences) at 1:10,000. Immunoblot quantification was performed by infrared imaging following the manufacturer's protocols using an Odyssey imaging system (Li-Cor Biosciences). All Odyssey images were processed using the Image J software (NIH) and assembled for presentation using Photoshop and Illustrator softwares (Adobe). For the experiments investigating the binding of GBAS-1 to GOA-1 in different activation states, His-GOA-1 was incubated in binding buffer supplemented with GDP (30 μM), GDP + AlF_4^- (30 μM GDP/30 μM $AlCl_3$/10 mM NaF) or GTPγS (30 μM) for 2.5 h at 30 °C right before the binding incubation with GST-GBAS-1. The wash buffer was also supplemented with the same nucleotides.

Protein Structure Homology Modeling and *In Silico* Mutagenesis Analyses

A homology model of nematode GOA-1 bound to a portion of GBAS-1 (GBA motif, aa 653–664) was generated from the X-ray crystal structure of human Gαi1 bound to the synthetic GEF peptide KB-752 (PDB: 1Y3A) using ICM Homology version 3.8-3 (Molsoft LLC., San Diego, CA). The GBAS-1 model was energetically minimized in the context of the GOA-1 structure using a Monte Carlo based approach (ICM, Molsfot LLC.), removed from the receptor, and redocked (Abagyan and Totrov 1994; Abagyan et al. 1994). Protein–protein docking of the GBAS-1 peptide to GOA-1 was conducted in silico using a two-stage fast Fourier transform

method (ICM, Molsfot LLC.) and compared with solutions from the ClusPro 2.0 server (Fernandez-Recio et al. 2002, 2003; Comeau et al. 2004; Kozakov et al. 2006). Simulations were carried out at 300 K in continuous dielectric solvent (no explicit waters). Prior to simulations, hydrogen atoms were populated and the isomeric/tautomeric state and positioning of side chains was optimized. The model was refined with a Fragment-Guided Molecular Dynamics simulation to improve local geometry by relaxing steric strains and to optimize torsion angles and hydrogen bonding networks (Zhang et al. 2011). Individual amino acid energy contributions to the stability of the modeled GOA-1:GBAS-1 complex and the effect of mutations on complex stability were calculated with FoldX version 3.0 (Guerois et al. 2002; Schymkowitz et al. 2005). Briefly, residues with unfavorable torsion, van der Waals clashes or high total energy were repaired and the per-residue energy contributions were obtained by calculating the difference ($\Delta\Delta G$) between monomeric GOA-1 (or free GBAS-1 peptide) and the GOA-1:GBAS-1 complex at the individual residue level. Monomeric forms were generated by manually removing GBAS-1 or GOA-1 from the repaired complex to assure stochastic differences in side-chain energies did not contribute to calculations. Mutational effects on the total stability of the complex were determined by building mutant protein models with flexible neighboring residues and calculating the difference in total energy from a corresponding native structure in which altered neighboring residues were positioned to match; the average of five models is reported to demonstrate convergence. Per-residue and mutation calculations in FoldX were for the system at pH 7.0, 0.05 M ionic strength, and 298 K. Model images were generated with PyMOL Molecular Graphics System, (Schrödinger, LLC.).

Steady-State GTPase Assay

This assay was performed as described previously (Garcia-Marcos et al. 2009, 2010; Garcia-Marcos, Kietrsunthorn, et al. 2011; Leyme et al. 2014). Briefly, His-GOA-1, His-Gαi3, or His-Gαo (100 nM) was preincubated with different concentrations of His-GBAS-1 (aa 631–758) for 15 min at 30 °C in assay buffer (20 mM Na-HEPES, pH 8, 100 mM NaCl, 1 mM EDTA, 25 mM $MgCl_2$, 1 mM DTT, 0.05% [w:v] $C_{12}E_{10}$). GTPase reactions were initiated at 30 °C by adding an equal volume of assay buffer containing 1 μM [γ-^{32}P]GTP (~50 c.p.m./fmol). For the time-course experiments, duplicate aliquots (50 μl) were removed at different time points and reactions stopped with 950 μl of ice-cold 5% (w/v) activated charcoal in 20 mM H_3PO_4, pH 3. For the dose-curve experiments, reactions were stopped at 15 min. Samples were then centrifuged for 10 min at 10,000 × g, and 500 μl of the resultant supernatant were scintillation counted to quantify released [^{32}P]Pi. For the time-course experiments, data were expressed as raw c.p.m. For the dose-curve experiments, the background [^{32}P]Pi detected at 15 min in the absence of G protein was subtracted from each reaction and data expressed as percentage of the Pi produced by His-GOA-1 in the absence of His-GBAS-1. Background counts were greater than 5% of the counts detected in the presence of G proteins.

GTPγS Binding Assay

GTPγS binding was measured using a filter binding method as described previously (Garcia-Marcos et al. 2010; Garcia-Marcos, Kietrsunthorn, et al. 2011; Aznar et al. 2015). His-GOA-1 (100 nM) was preincubated with different concentrations of His-GBAS-1 (631–758) for 15 min at 30 °C in assay buffer (20 mM Na-HEPES, pH 8, 100 mM NaCl, 1 mM EDTA, 25 mM $MgCl_2$, 1 mM DTT, 0.05% [w:v] $C_{12}E_{10}$). Reactions were initiated at 30 °C by adding an equal volume of assay buffer containing 1 μM [^{35}S] GTPγS (~50 c.p.m./fmol). For the time-course experiments, duplicate aliquots (25 μl) were removed at different time points, and binding of radioactive nucleotide was stopped by addition of 3 ml, ice-cold wash buffer (20 mM Tris–HCl, pH 8.0, 100 mM NaCl, 25 mM $MgCl_2$). For the dose-curve experiments, reactions were stopped at 15 min. The quenched reactions were rapidly passed through BA-85 nitrocellulose filters (GE Healthcare) and washed with 4 ml wash buffer. Filters were dried and subjected to liquid scintillation counting. For the time-course experiments, data were expressed as raw c.p.m. For the dose-curve experiments, the background [^{35}S]GTPγS detected in the absence of G protein was subtracted from each reaction and data expressed as percentage of the [^{35}S] GTPγS bound by His-GOA-1 in the absence of GBAS-1. Background counts were greater than 5% of the counts detected in the presence of G proteins.

Yeast Strains and Manipulations

The previously described (Cismowski et al. 1999) *Sa. cerevisiae* strain CY7967 [*MATα GPA1(1–41)-Gαi3 far1Δ fus1p-HIS3 can1 ste14:trp1:LYS2 ste3Δ lys2 ura3 leu2 trp1 his3*] (kindly provided by James Broach, Penn State University) was used for all experiments. The main features of this strain are that the only pheromone responsive GPCR (Ste3) is deleted, the endogenous Gα-subunit GPA1 is replaced by a chimeric GPA1(1–41)-human Gαi3 (36–354), and the cell cycle arrest-inducing protein *far1* is deleted. In this strain, the pheromone response pathway can be upregulated by the ectopic expression of activators of human Gαi3 and does not result in the cell cycle arrest that occurs in the native pheromone response (Cismowski et al. 1999, 2002). Plasmid transformations were carried out using the lithium acetate method. CY7967 was first transformed with a centromeric plasmid (CEN TRP) encoding for the LacZ gene under the control of the Fus1 promoter, which is activated by the pheromone response pathway. The P_{Fus1}::LacZ-expressing strain was transformed with derivatives of the pYES2 plasmid (2 μm, URA) encoding for GBAS-1 WT, GBAS-1 F660, or Ric-8A described in "Plasmid Constructs and Mutagenesis." Double transformants were selected in SD−TRP−URA media. Individual colonies were inoculated into 3 ml of SDGalactose−TRP−URA and incubated overnight at 30 °C to induce the expression of the proteins of interest under the control of a galactose-inducible promoter of pYES2. This starting culture was used to inoculate 20 ml of SDGalactose−TRP−URA at 0.3 OD_{600}. Exponentially growing cells (~0.7–0.8 OD_{600}, 4–5 h) were pelleted to prepare samples for subsequent assays (see

"Yeast Protein Immunoblotting" and "β-Galactosidase Activity Assay").

Yeast Protein Immunoblotting

This assay was performed as described previously (Cox et al. 1997; Hoffman et al. 2002) with minor modifications. Briefly, pellets corresponding to 5 OD_{600} were washed once with PBS + 0.1% bovine serum albumin (BSA) and resuspended in 150 µl of lysis buffer (10 mM Tris–HCl, pH 8.0, 10% [w:v] trichloroacetic acid, and 25 mM NH_4OAc, 1 mM EDTA); 100 µl of glass beads was added to each tube and vortexed at 4 °C for 5 min. Lysates were separated from glass beads by poking a hole in the bottom of the tubes followed by centrifugation onto a new set of tubes. The process was repeated after the addition of 50 µl of lysis buffer to wash the glass beads. Proteins were precipitated by centrifugation (10 min, 20,000 × g) and resuspended in 60 µl of solubilization buffer (0.1 M Tris–HCl, pH 11.0, 3% SDS). Samples were boiled for 5 min, centrifuged (1 min, 20,000 × g) and 50 µl of the supernatant transferred to new tubes containing 12.5 µl of Laemmli sample buffer and boiled for 5 min. Proteins (~15–20 µl per lane) were separated by SDS-PAGE, blocked in PBS supplemented with 5% BSA, and analyzed by sequential incubation with primary and secondary antibodies. Primary antibodies were diluted as follows: ppERK (rabbit mAb, Cell Signaling #4370), which recognizes yeast ppFus3: 1:2,500, myc (mouse mAb, Cell Signaling #9B11): 1:1,000, and α-tubulin (Sigma T6074): 1:2,500. Secondary antibodies (Goat anti-mouse IRDye 800 F(ab′)2, Li-Cor Biosciences, and Goat anti-rabbit Alexa Fluor 680, Lifetechnologies) were used at 1:10,000. Images were acquired in an Odyssey infrared scanner (Li-Cor), processed using the Image J software (NIH), and assembled for presentation using Photoshop and Illustrator softwares (Adobe).

β-Galactosidase Activity Assay

This assay was performed as described previously (Hoffman et al. 2002) with minor modifications. Pellets corresponding to 0.5 OD_{600} were washed once with PBS + 0.1% BSA and resuspended in 200 µl assay buffer (60 mM Na_2PO_4, 40 mM NaH_2PO_4, 10 mM KCl, 1 mM $MgCl_2$, 0.25% [v:v] β-mercaptoethanol, 0.01% [w:v] SDS, 10% [v:v] chloroform) and vortexed; 100 µl was transferred to 96-well plates and reactions started by the addition of 50 µl the fluorogenic β-galactosidase substrate fluorescein di-β-D-galactopyranoside (100 µM final). Fluorescence (Ex 485 ± 10 nm/Em 528 ± 10 nm) was measured every 2 min for 90 min at 30 °C in a Biotek H1 synergy plate reader. Enzymatic activity was calculated from the slope of fluorescence (arbitrary units) versus time (min). At least three independent clones determined in duplicate were measured for each condition and the results normalized (fold activation) to the activity in controls (strains carrying an empty pYES2 plasmid).

Statistical Analyses

Each experiment was performed at least three times. Data shown are expressed as mean ± SEM or as one representative result out of each biological replicate. Statistical significance between various conditions was assessed with the Student's *t*-test. $P < 0.05$ was considered significant.

Supplementary Material

Supplementary figures S1–S3 and table S1 are available at *Molecular Biology and Evolution* online (http://www.mbe.oxfordjournals.org/).

Acknowledgments

This work was supported by National Institute of Health grant R01GM108733 (to M.G.-M.), by a postdoctoral fellowship from the Hartwell Foundation (to V.D.G.), and by National Institute of Health grant R01NS036918 (to M.R.K.). The authors thank S. Sprang (University of Montana), J. Sondek (UNC, Chapel Hill), and J. Broach (Penn State University) for providing reagents and P. Polgar (BU) for giving access to equipment.

References

Abagyan R, Totrov M. 1994. Biased probability Monte Carlo conformational searches and electrostatic calculations for peptides and proteins. *J Mol Biol*. 235:983–1002.

Abagyan R, Totrov M, Kuznetsov D. 1994. Icm—a new method for protein modeling and design—applications to docking and structure prediction from the distorted native conformation. *J Comput Chem*. 15:488–506.

Afshar K, Willard FS, Colombo K, Johnston CA, McCudden CR, Siderovski DP, Gonczy P. 2004. RIC-8 is required for GPR-1/2-dependent Galpha function during asymmetric division of *C. elegans* embryos. *Cell* 119:219–230.

Afshar K, Willard FS, Colombo K, Siderovski DP, Gonczy P. 2005. Cortical localization of the Galpha protein GPA-16 requires RIC-8 function during *C. elegans* asymmetric cell division. *Development* 132: 4449–4459.

Anantharaman V, Abhiman S, de Souza RF, Aravind L. 2010. Comparative genomics uncovers novel structural and functional features of the heterotrimeric GTPase signaling system. *Gene* 475:63–78.

Austin RJ, Ja WW, Roberts RW. 2008. Evolution of class-specific peptides targeting a hot spot of the Galphas subunit. *J Mol Biol*. 377: 1406–1418.

Aznar N, Midde KK, Dunkel Y, Lopez-Sanchez I, Pavlova Y, Marivin A, Barbazan J, Murray F, Nitsche U, Janssen KP, et al. 2015. Daple is a novel non-receptor GEF required for trimeric G protein activation in Wnt signaling. *Elife* 4:e07091.

Bastiani C, Mendel J. 2006. Heterotrimeric G proteins in *C. elegans*. *WormBook* 13:1–25.

Blumer JB, Oner SS, Lanier SM. 2012. Group II activators of G-protein signalling and proteins containing a G-protein regulatory motif. *Acta Physiol*. 204:202–218.

Brenner S. 1974. The genetics of *Caenorhabditis elegans*. *Genetics* 77:71–94.

Buchan DW, Minneci F, Nugent TC, Bryson K, Jones DT. 2013. Scalable web services for the PSIPRED Protein Analysis Workbench. *Nucleic Acids Res*. 41:W349–W357.

Cabrita LD, Dai W, Bottomley SP. 2006. A family of *E. coli* expression vectors for laboratory scale and high throughput soluble protein production. *BMC Biotechnol*. 6:12

Chase DL, Koelle MR. 2004. Genetic analysis of RGS protein function in *Caenorhabditis elegans*. *Methods Enzymol*. 389:305–320.

Cheever ML, Snyder JT, Gershburg S, Siderovski DP, Harden TK, Sondek J. 2008. Crystal structure of the multifunctional Gbeta5-RGS9 complex. *Nat Struct Mol Biol*. 15:155–162.

Cismowski MJ, Ma C, Ribas C, Xie X, Spruyt M, Lizano JS, Lanier SM, Duzic E. 2000. Activation of heterotrimeric G-protein signaling by a ras-related protein. Implications for signal integration. *J Biol Chem*. 275:23421–23424.

Cismowski MJ, Takesono A, Ma C, Lanier SM, Duzic E. 2002. Identification of modulators of mammalian G-protein signaling by functional screens in the yeast *Saccharomyces cerevisiae*. *Methods Enzymol*. 344:153–168.

Cismowski MJ, Takesono A, Ma C, Lizano JS, Xie X, Fuernkranz H, Lanier SM, Duzic E. 1999. Genetic screens in yeast to identify mammalian nonreceptor modulators of G-protein signaling. *Nat Biotechnol*. 17:878–883.

Coleman DE, Berghuis AM, Lee E, Linder ME, Gilman AG, Sprang SR. 1994. Structures of active conformations of Gi alpha 1 and the mechanism of GTP hydrolysis. *Science* 265:1405–1412.

Coleman DE, Lee E, Mixon MB, Linder ME, Berghuis AM, Gilman AG, Sprang SR. 1994. Crystallization and preliminary crystallographic studies of Gi alpha 1 and mutants of Gi alpha 1 in the GTP and GDP-bound states. *J Mol Biol*. 238:630–634.

Comeau SR, Gatchell DW, Vajda S, Camacho CJ. 2004. ClusPro: a fully automated algorithm for protein-protein docking. *Nucleic Acids Res*. 32:W96–W99.

Cox JS, Chapman RE, Walter P. 1997. The unfolded protein response coordinates the production of endoplasmic reticulum protein and endoplasmic reticulum membrane. *Mol Biol Cell*. 8:1805–1814.

Cuppen E, van der Linden AM, Jansen G, Plasterk RH. 2003. Proteins interacting with *Caenorhabditis elegans* Galpha subunits. *Comp Funct Genomics*. 4:479–491.

de Mendoza A, Sebe-Pedros A, Ruiz-Trillo I. 2014. The evolution of the GPCR signaling system in eukaryotes: modularity, conservation, and the transition to metazoan multicellularity. *Genome Biol Evol*. 6:606–619.

De Vries L, Zheng B, Fischer T, Elenko E, Farquhar MG. 2000. The regulator of G protein signaling family. *Annu Rev Pharmacol Toxicol*. 40:235–271.

Dohlman HG, Thorner J. 1997. RGS proteins and signaling by heterotrimeric G proteins. *J Biol Chem*. 272:3871–3874.

Dong MQ, Chase D, Patikoglou GA, Koelle MR. 2000. Multiple RGS proteins alter neural G protein signaling to allow *C. elegans* to rapidly change behavior when fed. *Genes Dev*. 14:2003–2014.

Drenan RM, Doupnik CA, Boyle MP, Muglia LJ, Huettner JE, Linder ME, Blumer KJ. 2005. Palmitoylation regulates plasma membrane-nuclear shuttling of R7BP, a novel membrane anchor for the RGS7 family. *J Cell Biol*. 169:623–633.

Enomoto A, Ping J, Takahashi M. 2006. Girdin, a novel actin-binding protein, and its family of proteins possess versatile functions in the Akt and Wnt signaling pathways. *Ann N Y Acad Sci*. 1086:169–184.

Felsenstein J. 1985. Confidence-limits on phylogenies—an approach using the bootstrap. *Evolution* 39:783–791.

Fernandez-Recio J, Totrov M, Abagyan R. 2002. Soft protein-protein docking in internal coordinates. *Protein Sci*. 11:280–291.

Fernandez-Recio J, Totrov M, Abagyan R. 2003. ICM-DISCO docking by global energy optimization with fully flexible side-chains. *Proteins* 52:113–117.

Garcia-Marcos M, Ghosh P, Ear J, Farquhar MG. 2010. A structural determinant that renders G alpha(i) sensitive to activation by GIV/girdin is required to promote cell migration. *J Biol Chem*. 285: 12765–12777.

Garcia-Marcos M, Ghosh P, Farquhar MG. 2009. GIV is a nonreceptor GEF for G alpha i with a unique motif that regulates Akt signaling. *Proc Natl Acad Sci U S A*. 106:3178–3183.

Garcia-Marcos M, Ghosh P, Farquhar MG. 2015. GIV/Girdin transmits signals from multiple receptors by triggering trimeric G protein activation. *J Biol Chem*. 290:6697–6704.

Garcia-Marcos M, Jung BH, Ear J, Cabrera B, Carethers JM, Ghosh P. 2011. Expression of GIV/Girdin, a metastasis-related protein, predicts patient survival in colon cancer. *FASEB J*. 25:590–599.

Garcia-Marcos M, Kietrsunthorn PS, Pavlova Y, Adia MA, Ghosh P, Farquhar MG. 2012. Functional characterization of the guanine nucleotide exchange factor (GEF) motif of GIV protein reveals a threshold effect in signaling. *Proc Natl Acad Sci U S A*. 109:1961–1966.

Garcia-Marcos M, Kietrsunthorn PS, Wang H, Ghosh P, Farquhar MG. 2011. G Protein binding sites on Calnuc (nucleobindin 1) and NUCB2 (nucleobindin 2) define a new class of G(alpha)i-regulatory motifs. *J Biol Chem*. 286:28138–28149.

Ghosh P, Beas AO, Bornheimer SJ, Garcia-Marcos M, Forry EP, Johannson C, Ear J, Jung BH, Cabrera B, Carethers JM, et al. 2010. A G{alpha}i-GIV molecular complex binds epidermal growth factor receptor and determines whether cells migrate or proliferate. *Mol Biol Cell*. 21:2338–2354.

Ghosh P, Garcia-Marcos M, Bornheimer SJ, Farquhar MG. 2008. Activation of Galphai3 triggers cell migration via regulation of GIV. *J Cell Biol*. 182:381–393.

Gilman AG. 1987. G proteins: transducers of receptor-generated signals. *Annu Rev Biochem*. 56:615–649.

Gotta M, Ahringer J. 2001. Distinct roles for Galpha and Gbetagamma in regulating spindle position and orientation in *Caenorhabditis elegans* embryos. *Nat Cell Biol*. 3:297–300.

Gotta M, Dong Y, Peterson YK, Lanier SM, Ahringer J. 2003. Asymmetrically distributed *C. elegans* homologs of AGS3/PINS control spindle position in the early embryo. *Curr Biol*. 13:1029–1037.

Guerois R, Nielsen JE, Serrano L. 2002. Predicting changes in the stability of proteins and protein complexes: a study of more than 1000 mutations. *J Mol Biol*. 320:369–387.

Hajdu-Cronin YM, Chen WJ, Patikoglou G, Koelle MR, Sternberg PW. 1999. Antagonism between G(o)alpha and G(q)alpha in *Caenorhabditis elegans*: the RGS protein EAT-16 is necessary for G(o)alpha signaling and regulates G(q)alpha activity. *Genes Dev*. 13:1780–1793.

Hess HA, Roper JC, Grill SW, Koelle MR. 2004. RGS-7 completes a receptor-independent heterotrimeric G protein cycle to asymmetrically regulate mitotic spindle positioning in *C. elegans*. *Cell* 119: 209–218.

Hoffman GA, Garrison TR, Dohlman HG. 2002. Analysis of RGS proteins in *Saccharomyces cerevisiae*. *Methods Enzymol*. 344:617–631.

Hofler C, Koelle MR. 2011. AGS-3 alters *Caenorhabditis elegans* behavior after food deprivation via RIC-8 activation of the neural G protein G alphao. *J Neurosci*. 31:11553–11562.

Johnston CA, Willard FS, Jezyk MR, Fredericks Z, Bodor ET, Jones MB, Blaesius R, Watts VJ, Harden TK, Sondek J, et al. 2005. Structure of Galpha(i1) bound to a GDP-selective peptide provides insight into guanine nucleotide exchange. *Structure* 13:1069–1080.

Jose AM, Bany IA, Chase DL, Koelle MR. 2007. A specific subset of transient receptor potential vanilloid-type channel subunits in *Caenorhabditis elegans* endocrine cells function as mixed heteromers to promote neurotransmitter release. *Genetics* 175:93–105.

Kearse M, Moir R, Wilson A, Stones-Havas S, Cheung M, Sturrock S, Buxton S, Cooper A, Markowitz S, Duran C, et al. 2012. Geneious Basic: an integrated and extendable desktop software platform for the organization and analysis of sequence data. *Bioinformatics* 28:1647–1649.

Kleuss C, Raw AS, Lee E, Sprang SR, Gilman AG. 1994. Mechanism of GTP hydrolysis by G-protein alpha subunits. *Proc Natl Acad Sci U S A*. 91:9828–9831.

Kozakov D, Brenke R, Comeau SR, Vajda S. 2006. PIPER: an FFT-based protein docking program with pairwise potentials. *Proteins* 65: 392–406.

Kriventseva EV, Rahman N, Espinosa, O, Zdobnov EM. 2008. OrthoDB: the hierarchical catalog of eukaryotic orthologs. *Nucleic Acids Res*. 36:D271–D275.

Krumins AM, Gilman AG. 2002. Assay of RGS protein activity in vitro using purified components. *Methods Enzymol*. 344:673–685.

Lee MJ, Dohlman HG. 2008. Coactivation of G protein signaling by cell-surface receptors and an intracellular exchange factor. *Curr Biol*. 18:211–215.

Leyme A, Marivin A, Casler J, Nguyen LT, Garcia-Marcos M. 2014. Different biochemical properties explain why two equivalent

Galpha subunit mutants cause unrelated diseases. *J Biol Chem*. 289:21818–21827.
Lopez-Sanchez I, Dunkel Y, Roh YS, Mittal Y, De Minicis S, Muranyi A, Singh S, Shanmugam K, Aroonsakool N, Murray F, et al. 2014. GIV/Girdin is a central hub for profibrogenic signalling networks during liver fibrosis. *Nat Commun*. 5:4451
Matsushita E, Asai N, Enomoto A, Kawamoto Y, Kato T, Mii S, Maeda K, Shibata R, Hattori S, Hagikura M, et al. 2011. Protective role of Gipie, a Girdin family protein, in endoplasmic reticulum stress responses in endothelial cells. *Mol Biol Cell*. 22:736–747.
McCudden CR, Willard FS, Kimple RJ, Johnston CA, Hains MD, Jones MB, Siderovski DP. 2005. G alpha selectivity and inhibitor function of the multiple GoLoco motif protein GPSM2/LGN. *Biochim Biophys Acta*. 1745:254–264.
Mendel JE, Korswagen HC, Liu KS, Hajdu-Cronin YM, Simon MI, Plasterk RH, Sternberg PW. 1995. Participation of the protein Go in multiple aspects of behavior in *C. elegans*. *Science* 267:1652–1655.
Morris AJ, Malbon CC. 1999. Physiological regulation of G protein-linked signaling. *Physiol Rev*. 79:1373–1430.
Mukhopadhyay S, Ross EM. 2002. Quench-flow kinetic measurement of individual reactions of G-protein-catalyzed GTPase cycle. *Methods Enzymol*. 344:350–369.
Natochin M, Gasimov KG, Artemyev NO. 2001. Inhibition of GDP/GTP exchange on G alpha subunits by proteins containing G-protein regulatory motifs. *Biochemistry* 40:5322–5328.
Oates ME, Romero P, Ishida T, Ghalwash M, Mizianty MJ, Xue B, Dosztanyi Z, Uversky VN, Obradovic Z, Kurgan L, et al. 2013. D(2)P(2): database of disordered protein predictions. *Nucleic Acids Res*. 41:D508–D516.
Obenauer JC, Cantley LC, Yaffe MB. 2003. Scansite 2.0: Proteome-wide prediction of cell signaling interactions using short sequence motifs. *Nucleic Acids Res*. 31:3635–3641.
Papasergi MM, Patel BR, Tall GG. 2015. The G protein alpha chaperone Ric-8 as a potential therapeutic target. *Mol Pharmacol*. 87:52–63.
Rosenbaum DM, Rasmussen SG, Kobilka BK. 2009. The structure and function of G-protein-coupled receptors. *Nature* 459:356–363.
Ross EM, Wilkie TM. 2000. GTPase-activating proteins for heterotrimeric G proteins: regulators of G protein signaling (RGS) and RGS-like proteins. *Annu Rev Biochem*. 69:795–827.
Sato M, Blumer JB, Simon V, Lanier SM. 2006. Accessory proteins for G proteins: partners in signaling. *Annu Rev Pharmacol Toxicol*. 46:151–187.
Schymkowitz J, Borg J, Stricher F, Nys R, Rousseau F, Serrano L. 2005. The FoldX web server: an online force field. *Nucleic Acids Res*. 33: W382–W388.
Segalat L, Elkes DA, Kaplan JM. 1995. Modulation of serotonin-controlled behaviors by Go in *Caenorhabditis elegans*. *Science* 267:1648–1651.
Siderovski DP, Willard FS. 2005. The GAPs, GEFs, and GDIs of heterotrimeric G-protein alpha subunits. *Int J Biol Sci*. 1:51–66.
Sprang SR. 1997. G protein mechanisms: insights from structural analysis. *Annu Rev Biochem*. 66:639–678.
Stefanakis N, Carrera I, Hobert O. 2015. Regulatory logic of pan-neuronal gene expression in *C. elegans*. *Neuron* 87:733–750.
Stols L, Gu M, Dieckman L, Raffen R, Collart FR, Donnelly MI. 2002. A new vector for high-throughput, ligation-independent cloning encoding a tobacco etch virus protease cleavage site. *Protein Expr Purif*. 25:8–15.
Studier FW. 2005. Protein production by auto-induction in high density shaking cultures. *Protein Expr Purif*. 41:207–234.
Tall GG, Krumins AM, Gilman AG. 2003. Mammalian Ric-8A (synembryn) is a heterotrimeric Galpha protein guanine nucleotide exchange factor. *J Biol Chem*. 278:8356–8362.
Tamura K, Stecher G, Peterson D, Filipski A, Kumar S. 2013. MEGA6: Molecular Evolutionary Genetics Analysis version 6.0. *Mol Biol Evol*. 30:2725–2729.
Tanis JE, Moresco JJ, Lindquist RA, Koelle MR. 2008. Regulation of serotonin biosynthesis by the G proteins Galphao and Galphaq controls serotonin signaling in *Caenorhabditis elegans*. *Genetics* 178:157–169.
Thomas CJ, Briknarova K, Hilmer JK, Movahed N, Bothner B, Sumida JP, Tall GG, Sprang SR. 2011. The nucleotide exchange factor Ric-8A is a chaperone for the conformationally dynamic nucleotide-free state of Galphai1. *PLoS One* 6:e23197.
Wang H, Misaki T, Taupin V, Eguchi A, Ghosh P, Farquhar MG. 2014. GIV/girdin links vascular endothelial growth factor signaling to Akt survival signaling in podocytes independent of nephrin. *J Am Soc Nephrol*. 26:314–327.
Whelan S, Goldman N. 2001. A general empirical model of protein evolution derived from multiple protein families using a maximum-likelihood approach. *Mol Biol Evol*. 18:691–699.
Willard FS, Kimple RJ, Siderovski DP. 2004. Return of the GDI: the GoLoco motif in cell division. *Annu Rev Biochem*. 73:925–951.
Zhang J, Liang Y, Zhang Y. 2011. Atomic-level protein structure refinement using fragment-guided molecular dynamics conformation sampling. *Structure* 19:1784–1795.